

Interpreting the Information in Ozone Observations and Model Predictions Relevant to Regulatory Policies in the Eastern United States



Christian Hogrefe,^{*} S. Trivikrama Rao,^{*,+} Igor G. Zurbenko,⁺ and P. Steven Porter^{+,#}

ABSTRACT

To study the underlying forcing mechanisms that distinguish the days with high ozone concentrations from average or nonepisodic days, the observed and model-predicted ozone time series are spectrally decomposed into different temporal components; the modeled values are based on the results of a three-month simulation with the Urban Airshed Model—Variable Grid Version photochemical modeling system. The ozone power spectrum is represented as the sum of four temporal components, ranging from the intraday timescale to the multiweek timescale. The results reveal that only those components that contain fluctuations with periods equal to or greater than one day carry the information that distinguishes ozone episode days from nonepisodic days. Which of the longer-term fluctuations is dominant in a particular episode varies from episode to episode. However, the magnitude of the intraday fluctuations is nearly invariant in time. The promulgation of the 8-h standard for ozone further emphasizes the importance of longer-term fluctuations embedded in ozone time series data. Furthermore, the results indicate that the regional photochemical modeling system is able to capture these features. This paper also examines the effect of simulation length on the predicted ozone reductions stemming from emission reductions. The results demonstrate that for regulatory purposes, model simulations need to cover longer time periods than just the duration of a single ozone episode; this is necessary not only to perform a meaningful model performance evaluation, but also to quantify the variability in the efficacy of an emission control strategy.

1. Introduction

During summertime, ground-level concentrations of ozone frequently exceed the National Ambient Air Quality Standard (NAAQS) for 1-h ozone over a large portion of the northeastern United States. Currently,

emission reductions required to comply with the ozone NAAQS are being determined by applying three-dimensional, regional-scale, grid-based photochemical models to historical ozone episodic events that typically last 2–5 days (Tesche et al. 1996; Russell and Dennis 2000). In such an approach, simulations with varying emission reduction scenarios but the same meteorological conditions are carried out to address how a particular ozone episode could have been mitigated. The results from a few of these episodic simulations are often used to make more general statements about the efficacy of a certain emission control strategy for a given region.

In this study, we present an approach to comparing observations and model outputs that focuses on the timescales that are being resolved by the photochemical models. The concept of scale analysis is widely used for research in physical sciences, including meteorology, climatology, and air pollution (Goody et al. 1998; Salcedo et al. 1999). In recent years, several investigators have applied this concept to the analysis

^{*}Department of Earth and Atmospheric Sciences, The University at Albany, State University of New York, Albany, New York.

⁺Department of Biometry and Statistics, School of Public Health, The University at Albany, State University of New York, Rensselaer, New York.

[#]Department of Civil Engineering, University of Idaho, Idaho Falls, Idaho.

Corresponding author address: Dr. S. T. Rao, Office of Science and Technology, Room 198, New York State Department of Environmental Conservation, 50 Wolf Road, Albany, NY 12233-3259.

E-mail: strao@air.dec.state.ny.us

In final form 22 February 2000.

©2000 American Meteorological Society

and interpretation of the observed ground-level ozone concentrations in an attempt to better understand the ozone process (Rao et al. 1997; Vukovich 1997; Milanchus et al. 1998). While these studies used different approaches to perform the scale analysis, they demonstrated the need to separate the ozone time series into different temporal components to identify processes that affect ambient ozone concentrations. For example, Vukovich (1997) showed that a combination of interannual and synoptic-scale forcings caused a large number of days with high ozone concentration for large regions in the eastern United States. Rao et al. (1997) and Rao et al. (1998) showed that the synoptic component of ozone demonstrates the regionality of the ozone problem, and that changes in the long-term component of ozone, the trend, due to the implementation of emission control strategies can only be detected when seasonality is removed (Porter et al. 2000). However, these studies did not explicitly address the implications of their results to the use of photochemical models.

Initially, photochemical box models were used to study urban air quality (e.g., McRae and Seinfeld 1983). Subsequently, grid-based photochemical models such as the Regional Oxidant Model (Lamb 1983), the Urban Airshed Model with the Carbon Bond IV mechanism (U.S. Environmental Protection Agency 1990), and the Urban Airshed Model, Variable-Grid Version (UAM-V) (Systems Applications International 1995) were used in regional-scale air quality studies. Typically, only a few episodic days were simulated for limited regional domains (e.g., Hanna et al. 1996). As part of the Ozone Transport Assessment Group (OTAG) modeling activities, photochemical models were applied to a domain covering the eastern United States for simulation periods of up to 10 days to investigate the role of ozone transport. Also, analysis of observational data as part of the OTAG activities revealed the regional nature of the ozone problem in the eastern United States (Porter et al. 1996; OTAG 1997). Another reason for the interest in longer-term modeling is related to the 8-h NAAQS for ozone.

In this paper, we compare observations and photochemical modeling results from a simulation that was carried out continuously for the three summer months (June–August) of 1995. Because of the long modeling period, we are able to construct the ozone power spectrum and define intraday, diurnal, synoptic, and long-term timescales embedded in ozone time series. With traditional 2–3-day episodic modeling, we

can barely resolve the intraday and diurnal timescales and cannot resolve any longer timescales. We show that timescales greater than diurnal need to be considered in order to understand the nature of the ozone problem, to evaluate model performance on different timescales, and to quantify the efficacy of emission control strategies. We also discuss the importance of extended simulation periods when applying photochemical models in a regulatory setting and demonstrate that the shift from the 1- to the 8-h ozone NAAQS increases the importance of longer-term timescales.

2. Databases and method of analysis

a. Databases

Ozone observations were extracted from the U.S. Environmental Protection Agency's (U.S. EPA) Aerometric Information Retrieval System (AIRS) database; modeled ozone concentrations were obtained from a seasonal simulation of the UAM-V (Systems Applications International 1995) for the time period 4 June–31 August, 1995, covering the eastern United States. The meteorological input for this simulation was prepared using the Regional Atmospheric Modeling System (RAMS3b), whose application to regional air quality simulations was discussed by Pielke and Uliasz (1998). Details on meteorological modeling with RAMS3b can be found in Lagouvardos et al. (1997). UAM-V was run with two nested grids; the outer grid at 36-km resolution extends from 26° to 47°N and 99° to 67°W, and the inner grid at 12-km resolution extends from 32° to 44°N and 92° to 69.5°W. Fourteen vertical layers extend from the surface to about 4 km in the UAM-V model. The emission inventories used here have been described by Rao et al. (2000). The performance of the modeling system used in this simulation has been evaluated in Rao et al. (2000) and Sistla et al. (2000, unpublished manuscript). Only the monitoring data from stations within the inner grid and model results from grid cells that contained observational sites are analyzed.

For our analysis of the effects of emission control strategies, three additional seasonal simulations of the RAMS/UAM-V system were used. For the first of these additional simulations, all anthropogenic nitrogen oxide (NO_x) emissions were uniformly reduced by 50% and all anthropogenic volatile organic compound (VOC) emissions were reduced by 25%. For the other two simulations, the vertical resolution of the UAM-

V was set to five layers for the outer grid and seven layers for the inner grid, and the two emission reduction scenarios reflect projected emissions for 2007 (referred to as the 2007 base case) and a case with reduced emissions (referred to as the 2007 budget case) (N. Meyer 1996, personal communication). The reduced emissions scenario is aimed at reducing the regional-scale transport of ozone and its precursors as identified in the OTAG process (OTAG 1997), especially by reducing NO_x emissions from point sources.

b. Definition of timescales and associated processes

Time series of atmospheric pollutant concentrations contain fluctuations occurring on many different timescales. However, the highest and lowest resolvable frequencies are dictated by the sampling interval and the length of the data record, respectively. Since we analyze hourly concentrations of both ozone observations and model predictions for a time period of three months, the shortest period that can be resolved is 2 h and the longest period is on the order of 30–40 days. Spectral analysis indicates that the single largest forcing in the hourly ozone time series data is the diurnal forcing having a period of 24 h (Rao et al. 1997). Because of its large energy, it is necessary to separate the diurnal signal from the time series. Additional frequency bands of interest are the intraday range (periods less than 12 h), the synoptic range (periods of 2–21 days), and longer-term fluctuations (i.e., baseline that contains periods longer than 21 days). While an approximate choice of these periods was based on physical considerations (the intraday component should include fast-acting, local-level processes; the diurnal component should be dominated by the 24-h periodicity; the synoptic component should contain fluctuations related to changing weather patterns; and the baseline should contain the low-frequency part of the signal), the actual choice of frequency ranges was made to minimize the covariance between the estimates of the different components. Details on the choice of filter parameters for the estimation of spectral components can be found in Eskridge et al. (1997) and Rao et al. (1997).

The atmospheric processes that contribute to intraday fluctuations of ozone include vertical mixing, local NO titration by fresh emissions, and ozone response to fast-changing emission patterns during morning and evening rush hours. In addition, variability, for example, in wind speed and actinic flux on this timescale also will affect the intraday component for

ozone. Diurnal fluctuations in ground-level ozone are associated with diurnal variation of the solar flux and the resulting differences between daytime photochemical production and nighttime removal of ozone. The variations of ozone on the synoptic scale are caused by the changing meteorological conditions such as the presence of a stagnant high pressure system or the passage of frontal systems. Changing meteorological conditions on the synoptic scale also will affect the synoptic ozone component through day-to-day variations in the mixing heights and the presence/absence of clouds. The baseline fluctuations are partially caused by the seasonal variation of the solar flux or larger-scale transport patterns, but in addition, contain processes that cannot be attributed to either synoptic or seasonal variations and either act slowly or cause a shift in the mean ozone concentration, for example, changes in deposition due to changes in surface properties (such as leaf area index, harvesting, or drought conditions).

c. Spectral decomposition

While any method that can cleanly decompose a time series into fluctuations characterizing the desired timescales can be applied, we used the Kolmogorov–Zurbenko (KZ) filter (Zurbenko 1986) here because of its powerful separation characteristics, simplicity, and ability to handle missing data. Since a detailed discussion of the KZ filter along with a comparison to other separation techniques can be found in Eskridge et al. (1997) and Rao et al. (1997), we present only the key features of the KZ separation technique.

The KZ filter is an iterated moving average filter: the output from a simple moving average is again subjected to the same moving average operation for a specified number of iterations. Thus, the KZ filter can be characterized by two parameters, the length of the moving average window, m , and the number of iterations, k . The KZ filter is a low-pass filter: the filtered time series contains low-frequency fluctuations while the difference between the original time series and the filtered time series (residuals) contains the high-frequency part of the time series. A bandpass filter is created by taking the difference between two filtered time series. The separation point (cutoff frequency) between the high-frequency and low-frequency component is a function of the filter parameters m and k (Rao et al. 1997). The components of interest in this study, namely, the intraday (ID), diurnal (DU), synoptic (SY), and baseline (BL) components, are estimated as follows:

$$\begin{aligned}
 ID(t) &= \ln[O_3(t)] - KZ_{3,3} \{ \ln[O_3(t)] \} \\
 DU(t) &= KZ_{3,3} \{ \ln[O_3(t)] \} - KZ_{13,5} \{ \ln[O_3(t)] \} \\
 SY(t) &= KZ_{13,5} \{ \ln[O_3(t)] \} - KZ_{103,5} \{ \ln[O_3(t)] \} \\
 BL(t) &= KZ_{103,5} \{ \ln[O_3(t)] \},
 \end{aligned} \tag{1}$$

where $KZ_{m,k}$ is the KZ filter with a window size of m hours and k iterations.

The transfer functions for the $KZ_{3,3}$, $KZ_{13,5}$, and $KZ_{103,5}$ filters, respectively, as a function of frequency are presented in Fig. 1. Frequencies that cannot be resolved in this analysis because of the limitations of the data record (i.e., periods shorter than 2 h and longer than about 30–40 days) are left unshaded in Fig. 1. The value of the transfer function at a given frequency represents the fraction of energy of an oscillation with that frequency that would be retained in the filtered time series. Consequently, the remaining fraction of energy would be present in the residuals. For example, we see that about 90% of the energy associated with a weekly oscillation would appear in the estimate of the synoptic component, while about 10% of the energy would be transferred to the estimated diurnal component. For an ideal separation, the transfer functions would be step functions, and the energy of any given fluctuation would appear in no more than one estimated component. In reality, however, the separated components are not completely orthogonal, and our choice of the filter parameters is based both on the desired separation between the components and minimization of the covariances between the components. In particular, it can be seen that our ability to examine the intraday component at one end of the spectrum and the baseline component at the other side of the spectrum is constrained due to the sampling interval (hourly measure-

ments) and the length of the data record (three-month duration). Therefore, a considerable amount of energy from the diurnal signal (about 10%) will be present in the intraday component.

Keeping these constraints in mind, the KZ filtering method permits us to study the ozone processes on separate timescales. However, this separation does not imply that these processes are independent. As an example, the effect of vertical mixing, which occurs on an intraday scale, on ground-level ozone is expected to be dependent on the level of the ozone concentration aloft, which can vary on the synoptic timescale (Zhang and Rao 1999). But this method does allow the timescales that are important in understanding the high ozone concentration levels on a regional scale, which is the object of this study, to be identified.

d. Log transform of data

Time series of ozone concentrations are log transformed prior to analysis to stabilize the variance of each component. Without a log transform, the variance of the residual intraday component would exhibit a strong unwanted diurnal structure. The logarithmic scale also has the benefit of being a proportional scale. Thus, by adding all components as defined in Eq. (1), the ozone process is represented as

$$\ln[O_3(t)] = ID(t) + DU(t) + SY(t) + BL(t), \tag{2}$$

where the intraday, diurnal, and synoptic components are zero-mean processes (filter residuals or created from bandpass filters). To obtain the actual ozone concentration in units of parts per billion (ppb) at any given time t , Eq. (2) can be rewritten as

$$O_3(t) = e^{ID(t)} e^{DU(t)} e^{SY(t)} e^{BL(t)}. \tag{3}$$

For example, inserting in expression (3) values of 0.10, 0.8, 0.1, and 3.4 of the ID, DU, SY, and BL components, respectively, which are typical afternoon values under a moderate synoptic and baseline forcing, yield an ozone value of 81 ppb, while values of 0.1, -0.8, 0.1, and 3.4 of the ID, DU, SY, and BL components, respectively, would yield an ozone concentration of 17 ppb at nighttime for the same ID, SY, and BL forcing. Since $\exp(x) \approx 1 + x$ for small values of x , the numeric values of a given zero-mean component (i.e., ID, DU, or SY), when multiplied by 100, can be thought of also as the approximate percentage increase (or decrease) of the ozone concentration due to this component over the concentration given by the prod-

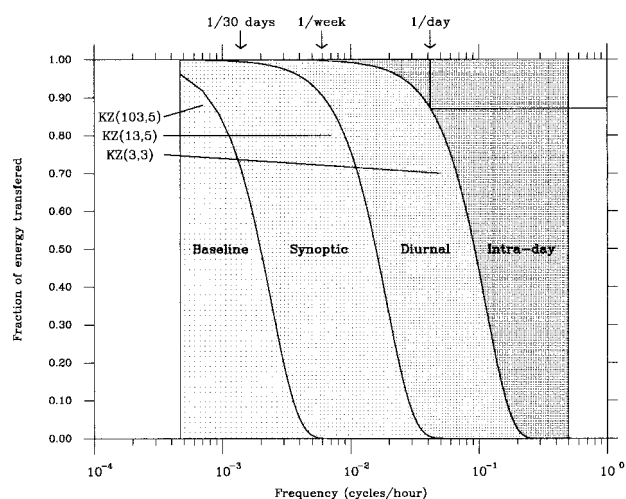


FIG. 1. Transfer functions for $KZ_{3,3}$, $KZ_{13,5}$, and $KZ_{103,5}$ filters.

uct of the exponents of the three other components. In the first example above, the product of the exponents of the BL, SY, and DU components would yield an ozone concentration of about 73 ppb, which is enhanced by the ID component by a factor of $\exp(0.1)$, or approximately 10%, to yield the total ozone concentration of 81 ppb. In this study, the values of the components in all figures are given both in the logarithmic scale on one axis and in the ppb scale on the other axis. While the values in the logarithmic scales are additive, the values in the ppb scale are multiplicative.

e. Methods of analysis

1) SPATIAL CORRELATION

To examine the spatial correlation structure of a given component, the correlation coefficient was computed for all possible pairs of monitoring sites or grid cells in the modeling domain. To calculate a correlation rose, the resulting correlation for each station pair was stored as a function of both distance and direction between the stations in 36 directional and 200 distance bins; the average correlation for each bin was calculated.

2) DAILY MAXIMUM OF 1-H OZONE

To investigate the relationship between the observed daily maximum 1-h ozone level and the strength of particular forcings on a given day, daily maximum 1-h ozone concentrations for all stations and days were classified according to the strength of the forcing. For the baseline and synoptic components, the daily mean was used as a surrogate for the strength of the forcing on that day, while for the diurnal and intraday component, the standard deviation over the 24-h period under consideration was used.

To eliminate the spatial variation in the absolute strength of the component forcings, each daily value for a given component was ranked with respect to the other 88 daily values of this component at the same station. Therefore, for each day of the season, the forcing of a given component is its $100(I/89)$ percentile value, where $I \in [1, 89]$ is the rank of the forcing compared to that of all other days. After repeating this procedure for all stations, the 1st, 25th, 50th (median), 75th and 99th percentiles of the distributions of the observed daily maximum ozone concentration for 10 different strengths of component forcings were calculated. For the first distribution, all daily maximum ozone values that occurred when the component forcing for that day was in the lower 10th percentile with

respect to the whole season were used; for the second distribution, all daily maximum ozone values that occurred when the component forcing for that day was between its 10th and 20th percentile with respect to the whole season were used; and so on. On average, each distribution contains about 5000 values. The characteristic features of these 10 distributions as a function of the strength of component forcing are displayed as box-whisker plots.

The relative strength of a component on a given day is defined as follows:

$$\begin{aligned} ID: & [e^{\sigma_{ID, \text{day}} - \sigma_{ID, \text{season}}} - 1] \times 100\% \\ DU: & [e^{\sigma_{DU, \text{day}} - \sigma_{DU, \text{season}}} - 1] \times 100\% \\ SY: & [e^{\overline{SY_{\text{day}}} - \overline{SY_{\text{season}}}} - 1] \times 100\% \\ BL: & [e^{\overline{BL_{\text{day}}} - \overline{BL_{\text{season}}}} - 1] \times 100\%. \end{aligned} \quad (4)$$

The relative strength reflects the percentage increase (or decrease) of observed ozone concentrations on a given day due to the strength of a particular forcing on that day relative to the average strength of that forcing.

3. Results and discussion

a. Ozone temporal components: Observations

The four estimated temporal components imbedded in ozone time series at the U.S. EPA AIRS station in Greenbelt, Maryland, are presented in Fig. 2. The stabilization of the variance resulting from the log transform is visible when the time series of the original and log-transformed ozone concentrations are compared. The time series of the intraday and diurnal components reveal little structure in this figure because the entire three-month period is displayed, and the resolution is not high enough to show the 89 diurnal cycles or the even higher-frequency oscillations in the intraday component; they are examined with higher resolution below. The synoptic and baseline components vary more slowly than the intraday and diurnal components; the synoptic component is predominant with periods on the order of 2–10 days, and the shortest period present in the baseline component is on the order of 2 weeks.

If the amplitudes of the four components in Fig. 2 are compared, it can be seen that the DU component has the largest amplitude, followed by the SY, BL, and ID components. This ranking is consistent with the finding that, averaged over all air monitoring stations, the ID, DU, SY, and BL components contain 7%, 68%,

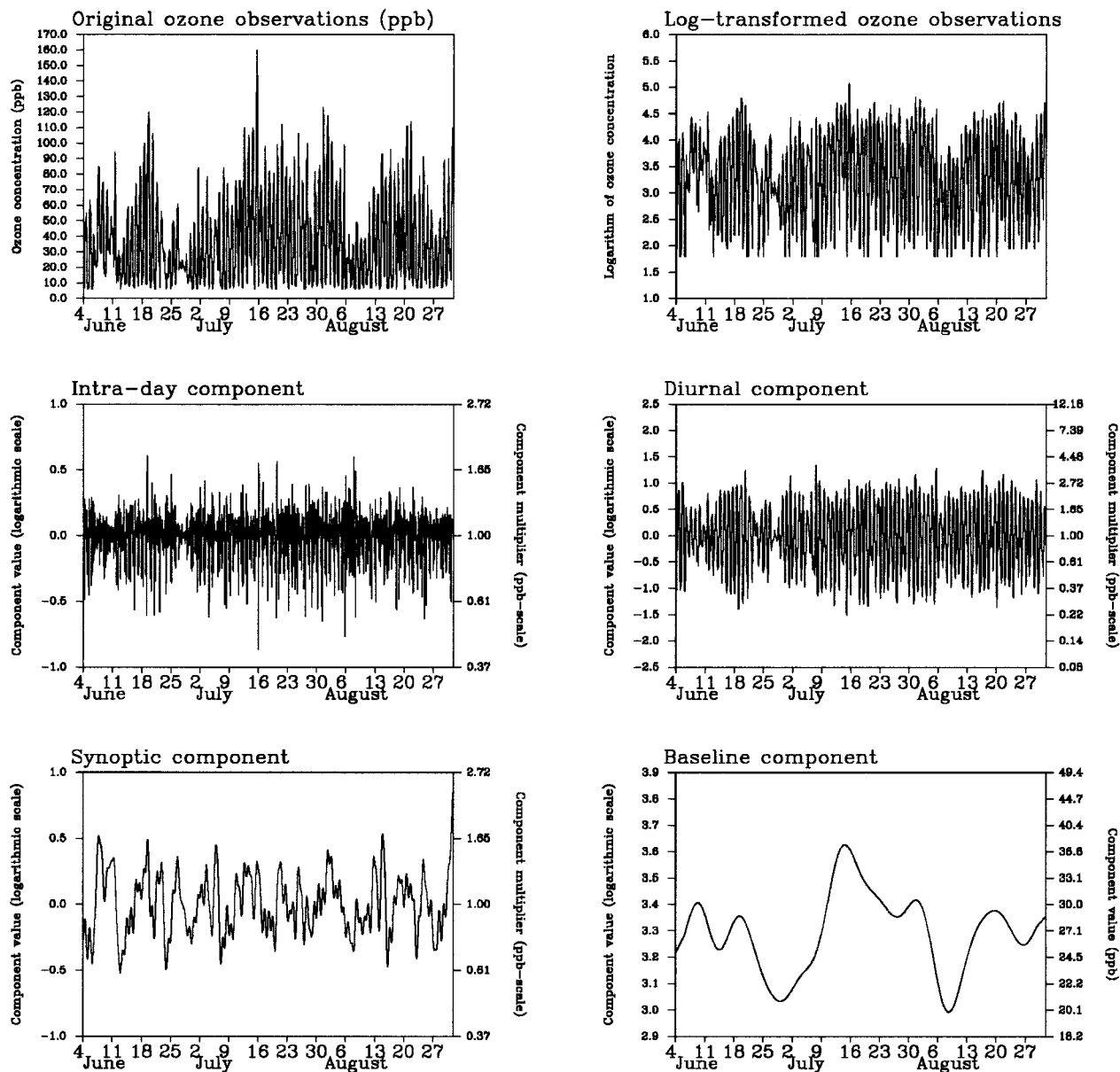


FIG. 2. Time series of observed hourly ozone concentrations, log-transformed observations, and the intraday, diurnal, synoptic, and baseline components for the period of 4 Jun 1995 to 31 Aug 1995 at Greenbelt, MD.

16%, and 9% of the total process energy (total variance), respectively.

Other features of interest in the ozone time series presented in Fig. 2 are the three major episodic events during the summer of 1995, which occurred around 19 June, 14 July, and 31 July. The days around these dates were characterized by high ozone concentrations over a large portion of the eastern United States. Although the behavior of different components during episodic and nonepisodic conditions will be examined in more detail later, it already can be noted that the intraday and diurnal components show local

maxima for only one of these three episodes (19 June), whereas the synoptic and baseline components show local maxima for all episodes.

As discussed in the previous section, the motivation for examining the ozone time series on different scales of motion was the notion that the processes affecting ozone occur on different (and nearly independent) timescales and, therefore, could be studied separately if the time series were spectrally decomposed. While time series analysis can never prove that the observed features are caused by a certain process or a combination of processes, it can provide evidence

in support of or against certain hypotheses. In the following, the intraday, diurnal, and synoptic components are discussed in more detail, focusing on the processes that affect these timescales.

The intraday component is displayed for a four-day period at a semiurban site (Greenbelt, Maryland) and a rural site (Trumbell Corners, New York) (Fig. 3a). This component displays little temporal structure at either site. One exception is the behavior of the intraday component in the morning hours [i.e., from 0600 to 1000 Eastern Standard time (EST)] that is observed at Greenbelt every day. This behavior probably is caused by the fast-changing emission patterns during the morning rush hour, resulting in initial removal of surface ozone by titration from fresh NO emissions. If the structure introduced by this morning hour behavior at the semiurban site is discounted, then the remaining structure is not systematic. Support for this explanation comes from the fact that no such behavior is observed at the rural location. Another feature that distinguishes the intraday time series at the two sites is that the magnitude of the fluctuations is much smaller at the rural location. This smaller magnitude at the rural site implies that ozone concentrations are not as affected by fast-varying emission patterns as at the urban site and are spatially more homogeneous. In addition to showing little temporal structure, time series of the intraday component also are nearly uncorrelated in space and do not show any significant correlation with any meteorological variable (Chan et al. 1999). Therefore, the intraday component is best described through its standard deviation at any given day as a measure of its strength. To properly describe

the fluctuations on the intraday scale, data with much higher temporal and spatial resolution would be needed.

The average diurnal cycles of the DU components for Greenbelt, Maryland, and Trumbell Corners, New York (Fig. 3b) show the smooth variation expected from the diurnal cycle associated with photochemical activity, vertical mixing, and removal processes.

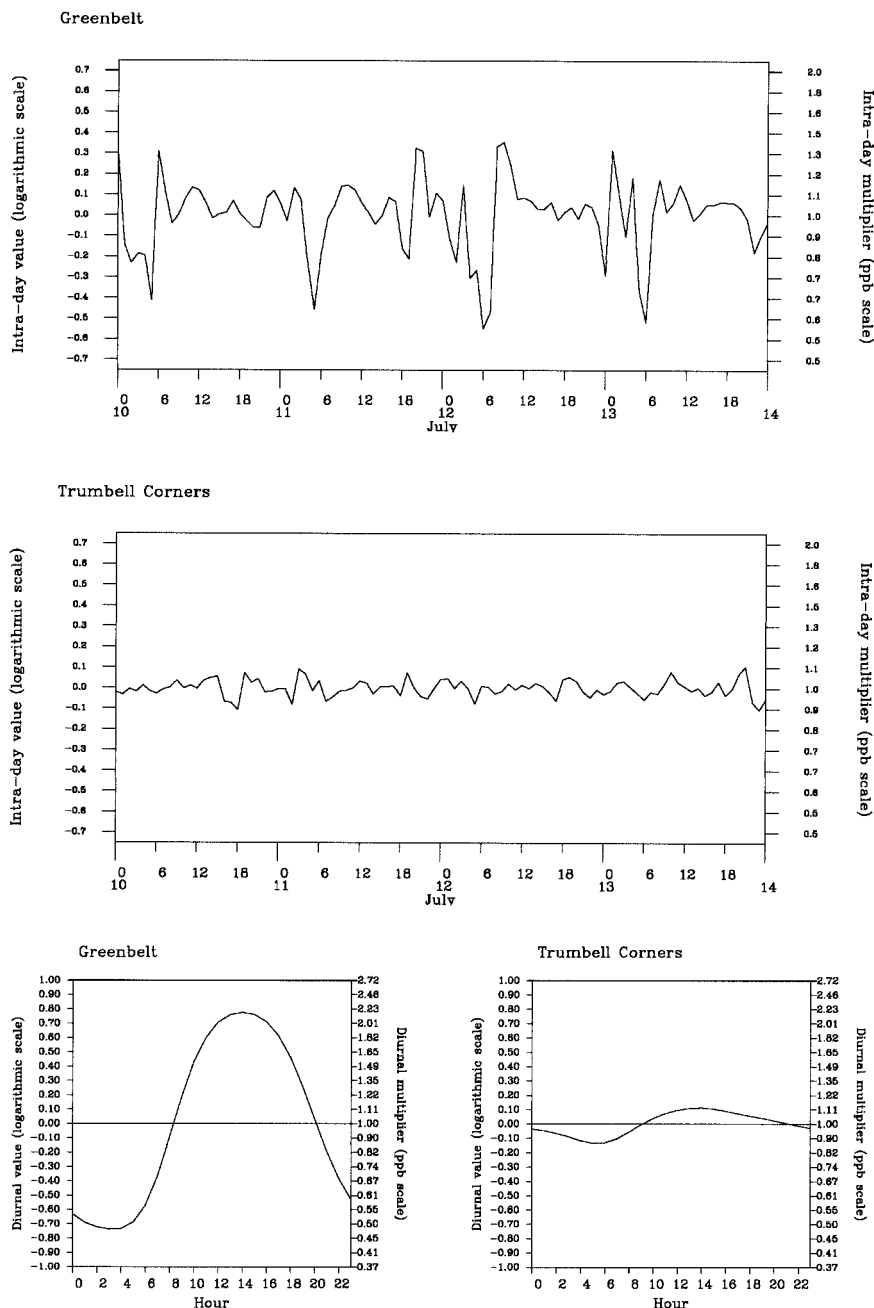


FIG. 3. (a) Time series of intraday component of 10 Jul 1995 to 13 Jul 1995 at Greenbelt, MD (urban), and Trumbell Corners, NY (rural). (b) Diurnal cycles of the diurnal component averaged over the summer season at Greenbelt, MD (urban), and Trumbell Corners, NY (rural). Times are EST.

The increase of ozone in the early morning hours (0600–1000 EST) is often dominated by downward mixing of high ozone concentrations aloft, while photochemical production is responsible for the further increase of ozone later despite the further growth of the mixed layer, which acts to dilute ground-level ozone concentrations (Zhang and Rao 1999). During nighttime, surface removal is responsible for the loss of ozone in the shallow nocturnal boundary layer in the absence of photochemical production. As with the ID component, it also can be seen that the range of fluctuations is about five times higher at the urban site than for the rural site, indicating less active photochemistry at the rural location. The information of most interest in the diurnal component is its amplitude on any given day, which is proportional to a day's standard deviation.

The SY component contains ozone fluctuations that are likely to be related to the change of prevailing meteorological conditions on the same timescale. If transport processes affect ozone concentrations, this effect also should be present in the synoptic component, since transport conditions vary with meteorological conditions (Brankov et al. 1998). The purpose of this section is to establish an *average* spatial scale for the synoptic ozone component, as defined in section 2e(1). As will be discussed in section 3e, this information is necessary to determine the required size of the modeling domain. In a previous study, Rao et al. (1997) found that correlations between the synoptic component at several urban reference locations and downwind locations had an *e*-folding distance of about 600 km along the direction of the prevailing wind. Their analysis used several years of daily maximum 1-h ozone concentrations rather than the 3-month hourly data used in this study, and, as a result, the definition of the SY component in their study is different. In a related study, Rao et al. (1998) found that the distance at which model-predicted changes in the maximum ozone concentrations stemming from emission reductions in a specific region drop to 37% of the maximum change is about 500 km along the direction of the prevailing wind. These studies, with their distinctions between different spatial axes and their focus on the relationship between the synoptic components downwind of major emission areas, suggested that the synoptic-scale effects on both emissions and ozone have a scale of up to 600 km.

In this study, the average spatial correlation of the synoptic component is presented by a correlation rose (Fig. 4) as described in section 2e(1). In this rose, the

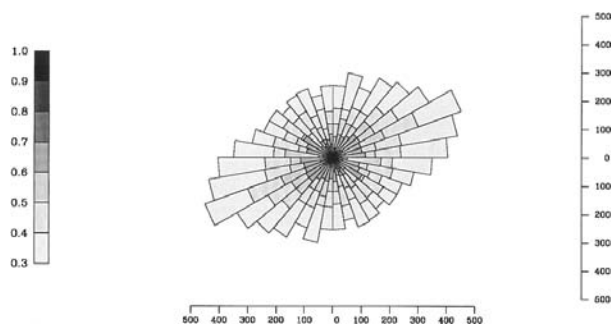


FIG. 4. Decay of correlation (left scale) as function of distance (km; right and bottom scales) and direction for the observed synoptic component.

distance between the correlated stations increases radially outward from the center of the rose, the segments represent different directions (with west to the left of the plot, east to the right, north to the top, and south to the bottom), and the shading represents the average correlation between the synoptic components at two stations at a given distance and direction. As noted above, this rose represents an *average* spatial correlation structure, since the reference location is not fixed (i.e., each station is used as reference station, and the rose is an average over all these reference stations). The average correlation structure shows directional dependence, with an *e*-folding distance of about 300 km in the SW–NE direction (the direction of the prevailing wind and the movement of other weather conditions) and about 200 km perpendicular to this direction. This directionality supports the notion by Rao et al. (1997, 1998) that atmospheric transport of ozone and its precursors is related to this observed spatial correlation structure. In addition, this average spatial scale of 200–300 km in hourly ozone data is much shorter than the one reported by Rao et al. (1997, 1998) for the synoptic component. While part of the smaller estimate in the present study is explained by the different definition of the synoptic component and the length of the data record analyzed, most of the difference can be explained by the fact that the results from Fig. 4 present an average over the entire modeling domain, whereas the estimates in Rao et al. (1997, 1998) were based on correlations with reference sites in major urban emission areas. In fact, a separate analysis (not shown here) reveals that the correlations of the synoptic components used in this study with the reference site in Greenbelt, Maryland, have an *e*-folding distance that is close to the estimate of 600 km reported by Rao et al. (1997, 1998).

b. Comparing episodic and nonepisodic daily maxima: Observations

From a regulatory standpoint, daily maximum ozone concentrations rather than hourly ozone time series are of interest. To investigate the relationship between the observed daily maximum ozone level and the strength of particular forcings for a given location and day, daily maximum ozone concentrations for all stations and days were classified according to the strength of the forcing using the method described in section 2e(2). In other words, while the daily maximum ozone concentration by definition is affected by each of the four components, we want to identify the timescales that show the strongest relationship between the strength of the forcing and observed maximum concentration. For the baseline and synoptic

components, their daily mean value was used as a surrogate for the strength of the forcing on that day, while for the diurnal and intraday components, their standard deviation over the 24-h period under consideration was used.

Figure 5 illustrates the results of such analysis for all four components. Box-whisker plots are used to represent the essential features (the white boxes indicate the medians, the black boxes the interquartile distance, and the whiskers extend to the 1st and 99th percentiles) of the 10 ozone distributions for different component forcings in each panel. The panels for the diurnal, synoptic, and baseline components all show a strong positive correlation between the strength of the forcing and observed daily maximum ozone concentrations. This correlation is observed for all as-

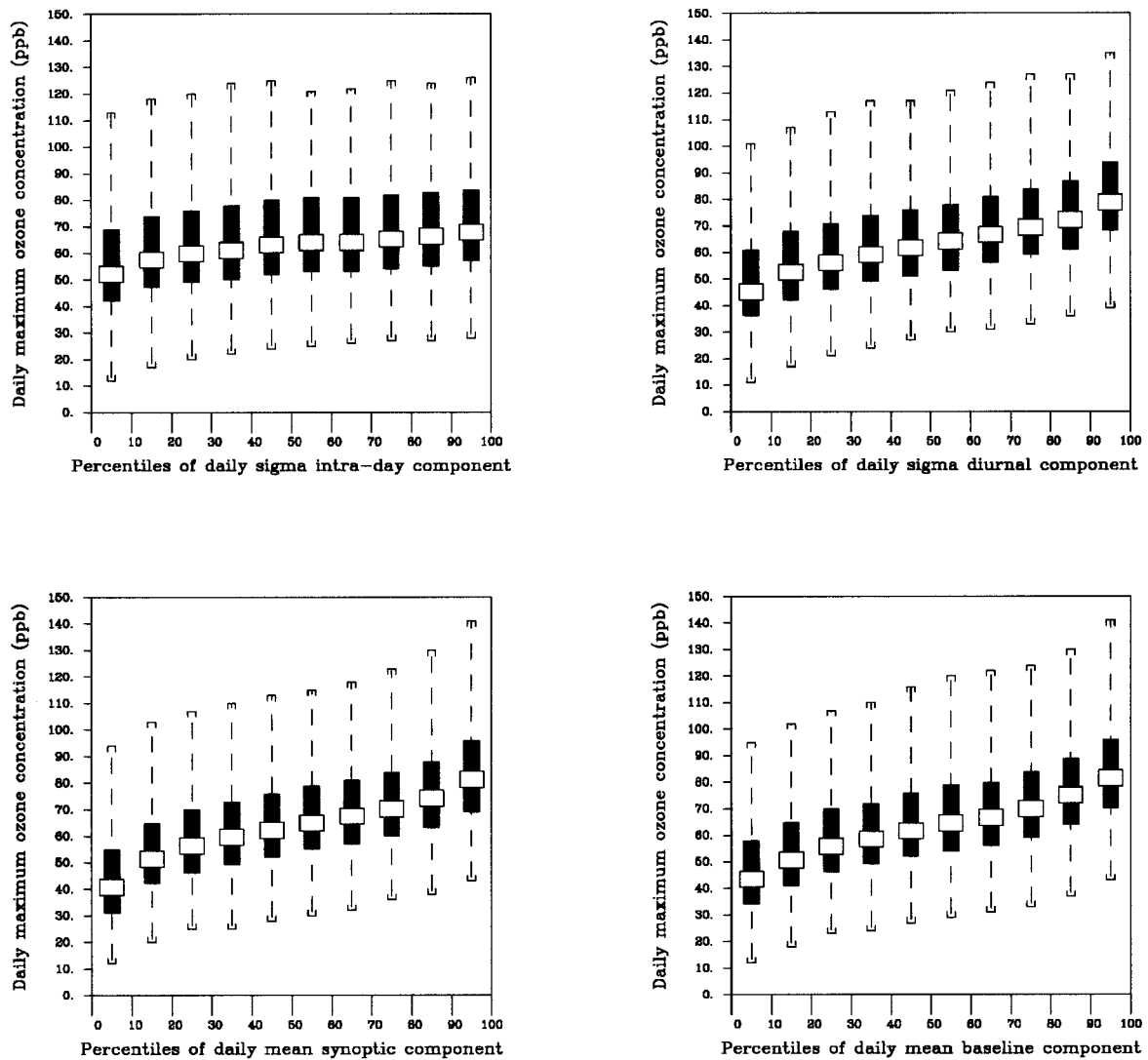


FIG. 5. Box-whisker plots for the distributions of observed daily maximum ozone concentrations as functions of the strength of a particular component on that day for all four components.

pects of the distributions, that is for the medians, interquartile distances, and 1st and 99th percentiles. It is a clear indication that the likelihood for high ozone concentrations increases as the strength of each of these forcings increase. Moreover, ozone concentrations in excess of 120 ppb are highly unlikely when any of these three forcings is very low, that is, below its 30th percentile.

On the other hand, the panel for the intraday component shows that the strength of the intraday forcing and daily maximum ozone values are only weakly correlated. In particular, the 99th percentile values for daily maximum ozone are almost independent of the strength of the intraday forcing for that day. The weakness of this correlation can be explained by the fact that the actual value of the intraday component at the hour of the daily maximum ozone concentration, while generally positive, is variable from day to day, and, therefore, a larger standard deviation of the intraday component on a given day does not necessarily lead to a larger value of the intraday component at the time of the daily maximum. However, some correlation is expected since a greater standard deviation of the intraday component increases the probability of a greater contribution from the intraday component to the ozone concentration at the hour of the daily maximum. These results indicate clearly that the strength of the diurnal, synoptic, and baseline forcings dictate the behavior of the daily maximum ozone concentration to a much greater degree than does the strength of the intraday component.

As noted in section 2e(2), deciles of relative component forcing rather than absolute values of component strength are used for this analysis because of the spatial differences in absolute component values. For illustration of how a particular ozone concentration of 120 ppb can result from different combinations of component forcings, especially from the diurnal, synoptic, and baseline components, consider the following example. At a given location, the mean maximum ozone concentration might be 55 ppb, reflecting mean afternoon values of 0.1, 0.6, 0.0, and 3.3 for the ID, DU, SY, and BL components, respectively [$\exp(0.1 + 0.6 + 0.0 + 3.3) \approx 55$ ppb]. Since, as shown in Fig. 5, the value of the intraday component is almost invariant in time, an ozone concentration of 120 ppb can be caused by higher diurnal and/or synoptic and/or baseline forcings. In other words, increased synoptic (0.4 instead of 0.0) and baseline (3.7 instead of 3.3) forcings with unchanged intraday and diurnal forcing can lead to an ozone concentration of 120 ppb as well

as a strong elevation of the diurnal component (1.1 instead of 0.6) with only slight elevation of the synoptic (0.2 instead of 0.0) and baseline (3.4 instead of 3.3) components, since $\exp(0.1 + 0.6 + 0.4 + 3.7) = \exp(0.1 + 1.1 + 0.2 + 3.4) \approx 120$ ppb.

To investigate the differences in the dynamical forcings that distinguish episodic and nonepisodic conditions, sample distributions of each of the observed four components at two sites for days with high ozone concentrations only (daily maximum ozone concentrations greater than 100 ppb) and for all days in the summer season (June, July, and August) are examined (Figs. 6a and 6b). The length of the data record used in this analysis is 18 yr for both Greenbelt, Maryland, and Flemington, New Jersey, locations. In addition to single sites having a long time record, sample distributions for the different components for only the summer season of 1995 were prepared, using data from all available observational sites and again distinguishing between the distributions for all days and only days with daily maximum ozone concentrations in excess of 100 ppb (Fig. 7). Differences between episodic and nonepisodic conditions are most evident in the synoptic and baseline components; there are slight differences in the diurnal component (Figs. 6 and 7). Most striking perhaps is that the ID component is virtually the same for episodic and nonepisodic days and has a very tight distribution with most values less than ± 0.15 . Both the positive mean value of the synoptic component and the upward shift of the mean baseline for the high-ozone-day distributions are evidence that high ozone concentrations tend to occur when the synoptic forcing is positive and the baseline forcing is stronger than average. This result implies that the longer-term processes (periods greater than a day) are the essential forcing mechanisms for high ozone concentration levels. (As discussed below, this conclusion also holds for model predictions carried out for the same time period).

To examine whether the above findings hold true in specific episodic situations, spatial images of the relative strength of the different temporal components over the eastern United States during several days of the 10–15 July episode, and the 30 July–2 August episode are presented in Figs. 8 and 9 along with images of the observed daily maximum ozone concentration for each day. The relative strength of a component on a given day is determined as defined by Eq. (4) in section 2e(2) and reflects the percentage increase (or decrease) of observed ozone concentrations due to the forcing on this day relative to the ozone concentration

that would be observed if the forcing were at its average level.

Figure 8 displays the results of this analysis for 14, 15, and 16 July 1995. The upper panel for each of the three days shows the observed ozone concentrations, and the panels below show the relative strength of the intraday, diurnal, synoptic, and baseline forcing for each day, respectively. It can be seen that daily maximum ozone concentrations in excess of 100 ppb were observed for large regions of the northeastern United States for 14 July. On 15 July, high ozone concentrations were observed for the entire Baltimore/Washington–New York City corridor, and the Pittsburgh and Atlanta regions. On 16 July, ozone concentrations were below 100 ppb in the entire domain. It is also evident that the additional contribution of the intraday component to observed ozone concentrations for each of these days was within $\pm 10\%$ of its average value. The diurnal component even had a 10%–30% lower contribution to daily maximum ozone concentrations for this episode than on average. Consequently, the increased ozone concentrations had to be caused by increased forcing from the longer-term components. Indeed, it can be seen that the baseline has increased between 30% and 70% for all regions in which high ozone concentrations were observed during this episode. On top of this elevated baseline, the synoptic component increased ozone concentrations by more than 60% relative to the average conditions for large regions of the northeastern United States on 14 and 15 July. On 16 July, after a cold front had passed through the northeast, the synoptic component was reduced considerably and, although the baseline level was still high, it was not sufficient to cause ozone exceedances. This result implies that, while the slowly varying baseline created favorable conditions for high ozone concentrations over a long time period (at least 10 days), the actual exceedances were observed only under a high synoptic forcing during this period of an already elevated baseline.

Similar analysis from the time period of 30 July–2 August 1995 (Fig. 9) reveals that high ozone concentrations were less widespread during this episode. Again, the additional contribution of the intraday component to observed ozone concentrations for each of these days was within $\pm 10\%$ of its average value. However, in contrast to the previous episode, the elevation of the baseline was not as widespread and strong (only between 10% and 30% for the urban corridor), and in addition to the strong elevation of the synoptic component, the diurnal forcing was also a

contributor to the observed high ozone concentrations. Thus, it can be seen that episodes differ from each other in terms of the relative contribution of the different components to high ozone concentrations. A common feature of the two episodes investigated here is the fact that the baseline is elevated and the synoptic component exerts a strong positive forcing, but there might be situations in which all of the positive forcing could be coming from the diurnal and/or synoptic components.

While fluctuations on the intraday timescale such as chemical reactions or mixing processes certainly represent important processes, the results of this section show that it is the longer-term components (diurnal, synoptic, and baseline) that provide essential information for understanding high ozone concentrations. This implies that even were data of increased temporal and spatial resolution available, it would not necessarily lead to a greater understanding of the longer-term processes that characterize the days of high ozone.

c. Comparing episodic and nonepisodic daily maxima: Model simulations

The analysis that produced Figs. 5 and 7 was repeated for UAM-V simulated hourly ozone concentrations at the grid cells corresponding to the observation sites used in the previous section. The box-whisker plots in Fig. 10 illustrate the relationship between the strength of a particular forcing and simulated daily maximum ozone values (cf. Fig. 5), and Fig. 11 shows the sample distributions of the temporal components of model results (cf. Fig. 7). The box-whisker plots illustrate that simulated ozone concentrations are correlated with the strength of diurnal, synoptic, and baseline forcing, and are independent of the strength of the intraday forcing. This behavior is similar to that of the observations, although the increase of the median daily maximum ozone with increasing diurnal forcing is weaker in the model predictions than in the observations, and the observations do display a weak correlation between the strength of intraday forcing and observed daily maximum concentrations. The sample distributions for the model agree with those for the observations in that high ozone days (when the simulated ozone concentrations exceeded 100 ppb) are characterized by an elevated baseline, positive synoptic forcing, and a slightly enhanced diurnal amplitude, while the distribution of the intraday component again remains virtually unchanged. Overall, the connection between positive forcings from processes having time-scales of a day or longer and high ozone concentrations

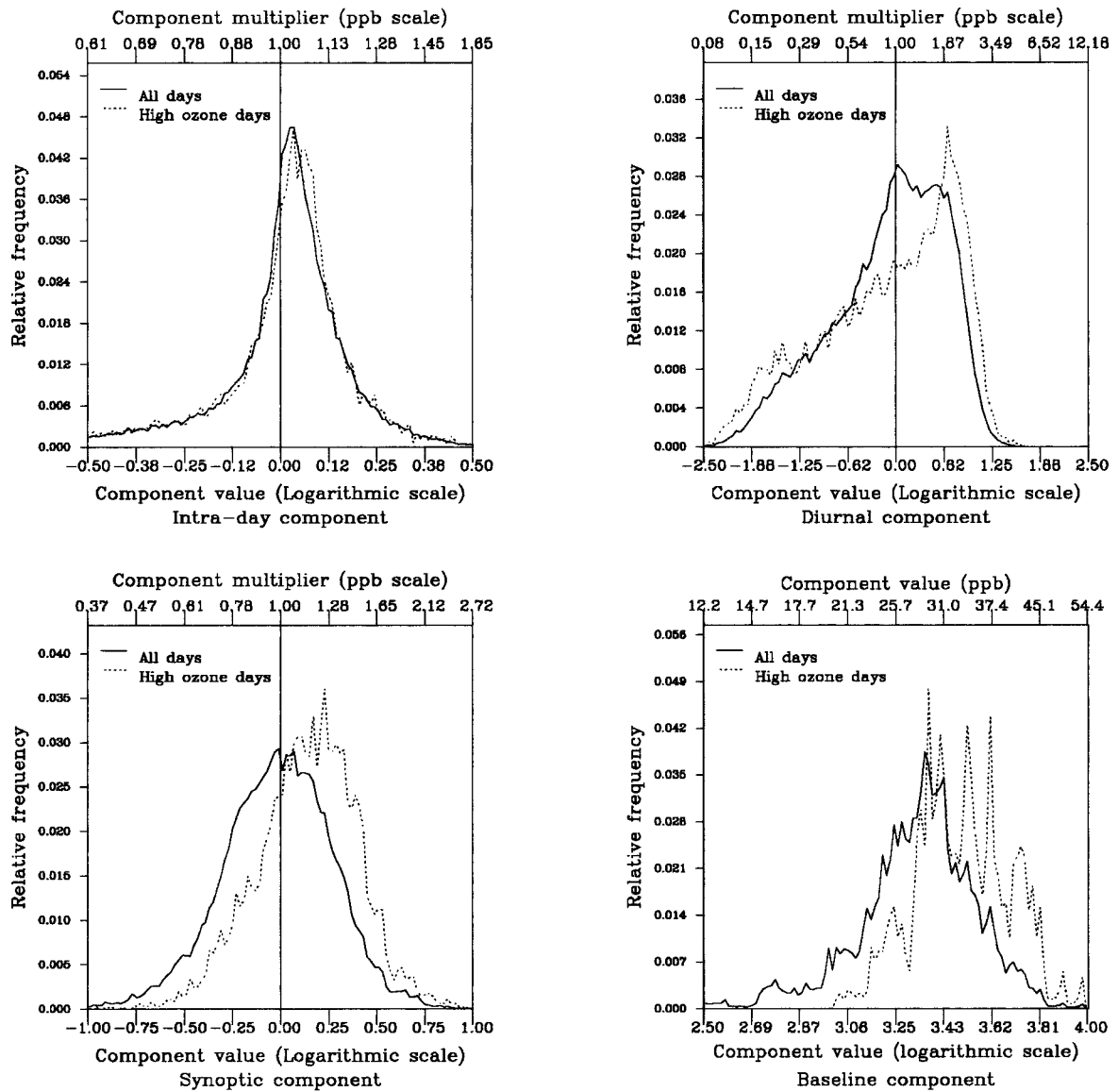


FIG. 6. (a) Sample distributions for the four components from 18 yr of observations at Greenbelt, MD, for both all summer days and summer days with ozone concentrations in excess of 100 ppb only.

appears to be captured well by the UAM-V modeling system. A detailed evaluation of UAM-V performance in simulating the observed ozone concentrations can be found in Rao et al. (2000) and Sistla et al. (2000, unpublished manuscript).

d. 1-h versus 8-h ozone standards

In 1997, the U.S. EPA promulgated the change of the NAAQS for ozone from the 1-h average to 8-h average ozone concentration. The threshold value for ozone exceedances was lowered from 120 ppb for the 1-h average concentration to 80 ppb for the 8-h average concentration. For the summer of 1995, the time series of the number of observation stations in the

modeling domain that exceeded the 1-h 120 ppb and 8-h 80 ppb standards on any given day was calculated (the resulting figure is not presented here because of space limitations). The results show that while both curves closely follow each other, the number of stations exceeding the 8-h standard at any given day is about *four* times larger than the number of stations exceeding the 1-h standard. In other words, the spatial extent of the ozone problem is considerably larger if consideration is given to the 8-h standard.

The 8-h standard is also likely to place a greater emphasis on ozone variations on longer timescales, since intraday variations are essentially smoothed out in a time series of 8-h moving average concentrations.

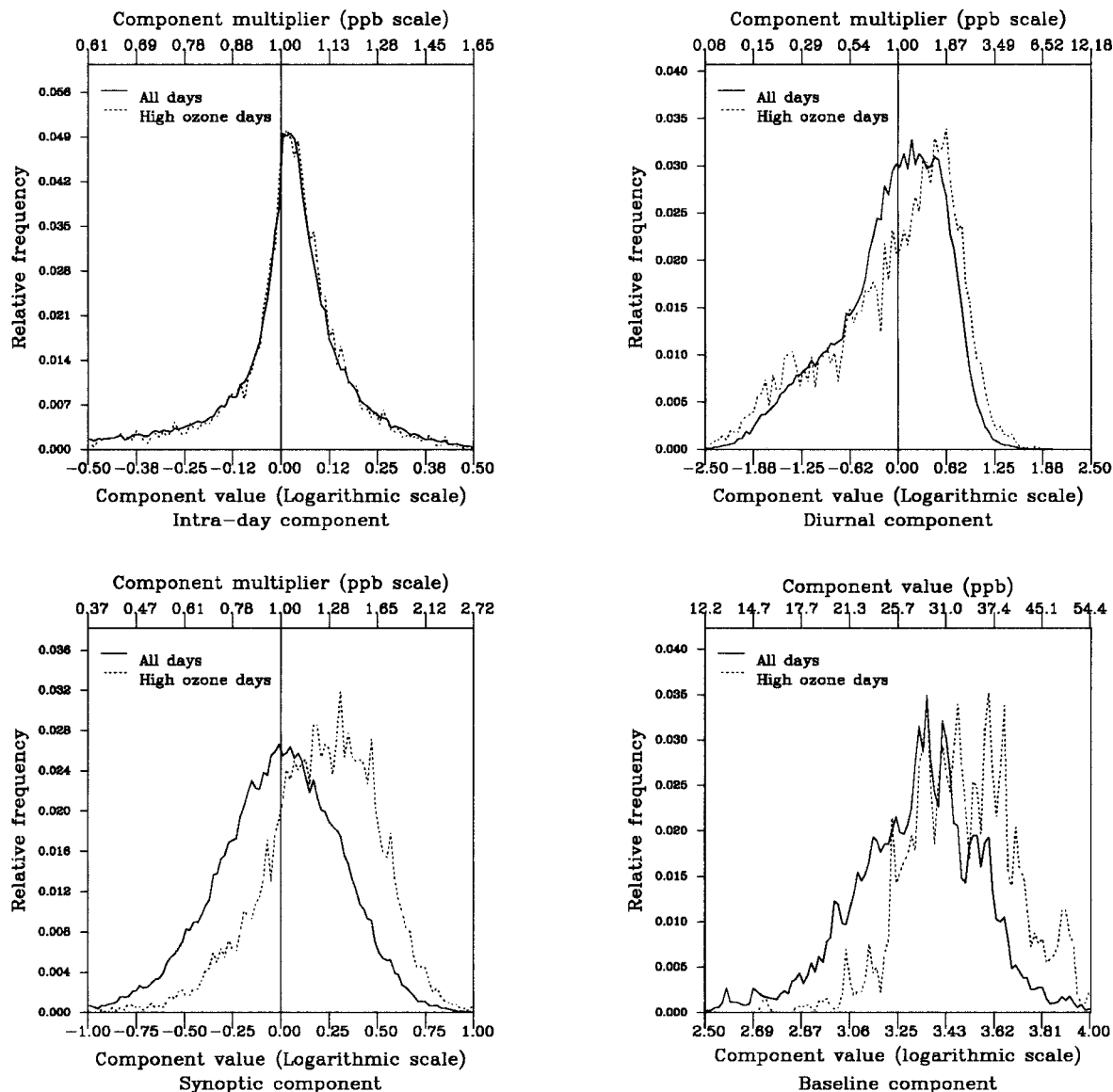


FIG. 6. (b) As in (a), but for Flemington, NJ.

To examine this hypothesis, we calculated the magnitude of the variations on the intraday, diurnal, synoptic, and baseline timescales for both the 1- and 8-h time series. To create the 8-h time series, a moving 8-h average filter was applied to the raw (not log transformed) hourly ozone time series, the resulting hourly values of 8-h average concentrations were then log transformed and decomposed as described in section 2c. The absolute standard deviations of the baseline and synoptic components remained virtually unchanged, whereas the absolute standard deviations of the diurnal and especially intraday component were reduced for the time series of 8-h concentrations. Consequently, the relative importance of each of the components is shifted as illustrated in Table 1. For 1-h concentrations,

the ID, DU, SY, and BL components contribute about 7%, 68%, 16%, and 9% of the total variance, respectively. For 8-h concentrations, these contributions are 1%, 64%, 22%, and 13%, respectively. This result implies that it is even more important to consider fluctuations occurring on the synoptic and baseline timescales when examining the 8-h average ozone concentrations with a photochemical model.

The transition from the 1-h standard to the 8-h standard also has implications for the duration of ozone episodes, and, consequently, to the length of simulations of photochemical models. One way of illustrating this effect is to determine the maximum number of consecutive days that have the potential of exceeding the ozone standard. Based on the analysis

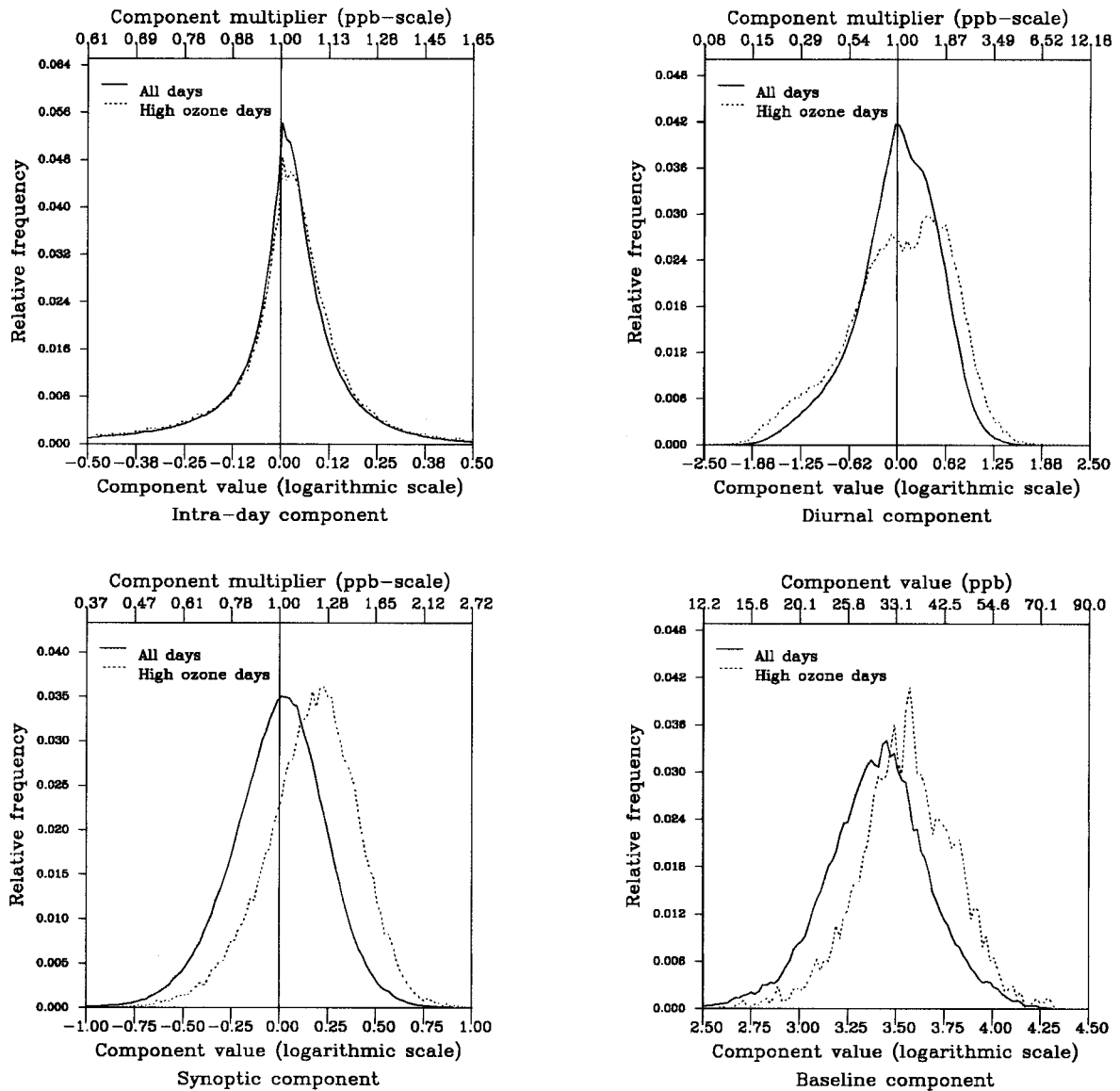


FIG. 7. As in Fig. 6a, but using observations from all stations in the modeling domain for the summer of 1995 only.

TABLE 1. Relative contributions of the intraday, diurnal, synoptic, and baseline components to the overall variance for hourly time series of 1- and 8-h average ozone concentrations (spatial average).

	Time series of hourly 1-h average ozone concentrations	Time series of hourly 8-h average ozone concentrations
Intraday component	7%	1%
Diurnal component	68%	65%
Synoptic component	16%	21%
Baseline component	9%	13%

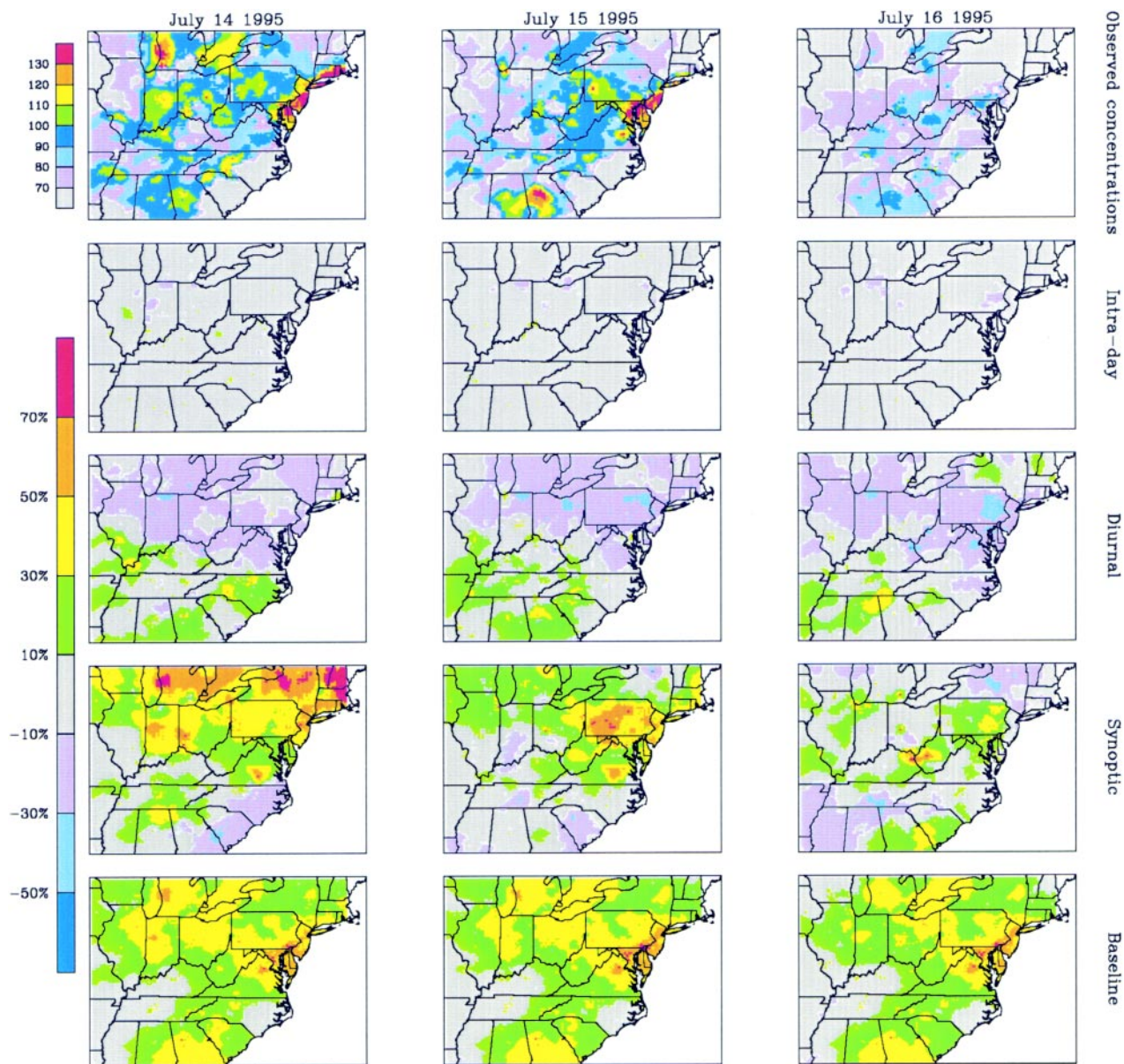


FIG. 8. Observed ozone concentrations (ppb) and relative strengths of component forcings for 14, 15, and 16 Jul 1995.

presented above, such a potential could be defined as the ozone concentration 20% below the ozone standard, since on such days a synoptic forcing of +0.25 (or about +25%) would lead to ozone exceedances [cf. Eq. (3)], and this value is the typical mean synoptic forcing on high ozone concentration days. Figure 12 shows the results of this estimate for the 1- and 8-h standards. It can be seen that for the 1-h values, the maximum number of consecutive days that have the potential of exceeding the standard is 6, while for the 8-h values this number exceeds 14 for the Atlanta area and for some locations in the northeastern urban corridor. This result demonstrates the need

for modeling for longer periods when considering the 8-h standard. It has to be noted that this estimate of the maximum number of days having an ozone exceedance potential is not quite realistic, since in reality a combination of forcings can contribute to high ozone concentrations, and these processes are nonlinear when one works in the ppb scale. Therefore, these results should be viewed only qualitatively.

e. Implications for model applications

The correlations between observed and model-simulated ozone concentration are insignificant on the intraday scale but high for the synoptic and baseline

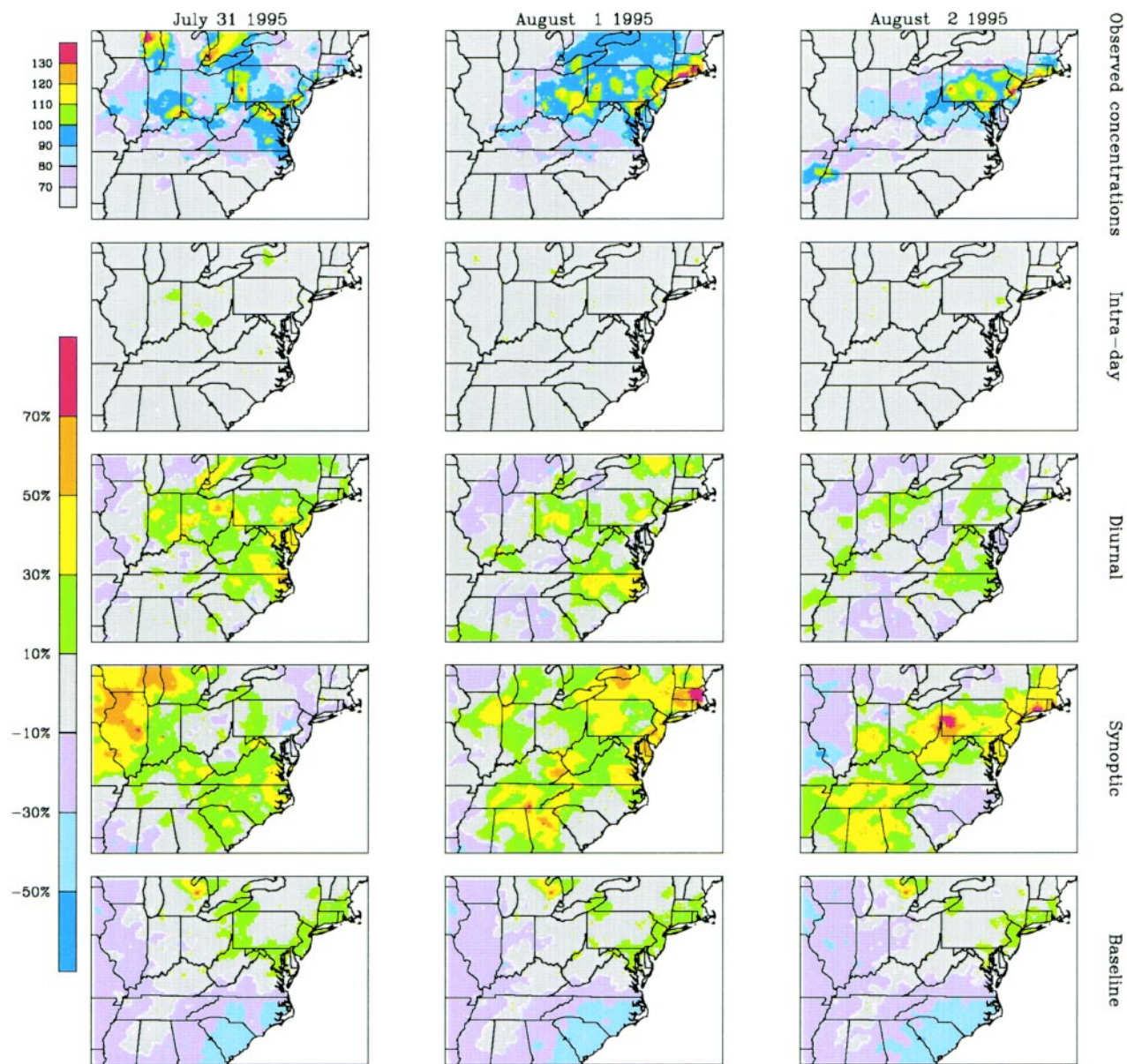


FIG. 9. As in Fig. 8, but for 31 Jul, 1 Aug, and 2 Aug 1995.

components (Hogrefe et al. 1999b; Rao et al. 2000); and, as discussed above, processes with timescales from 1 day to several weeks are tied more closely to ozone episodes than are processes with shorter timescales. Therefore, when photochemical models are used for regulatory purposes, model simulations for periods longer than the traditional 2–3 episodic days are needed.

In addition, since longer timescales imply larger spatial scales, the regional-scale processes that are reflected in those timescales must be actually modeled and not prescribed by the boundary conditions. As discussed in section 3a, the spatial scale of synoptic-scale transport can be on the order of up to 600 km

downwind of major emission regions. Therefore, the modeling domain should be at least four times as large as this spatial scale (or 2000–2500 km) in order to simulate these effects.

In addition to this requirement for the modeling domain of interest (the inner grid of a nested model), the outer model grid should be large enough to minimize the effect of boundary conditions.

The modeled time period has to be long enough to simulate the longer-term fluctuations responsible for high ozone concentrations. In addition, model evaluation should be performed over more than one synoptic cycle. For the synoptic scale, which contains

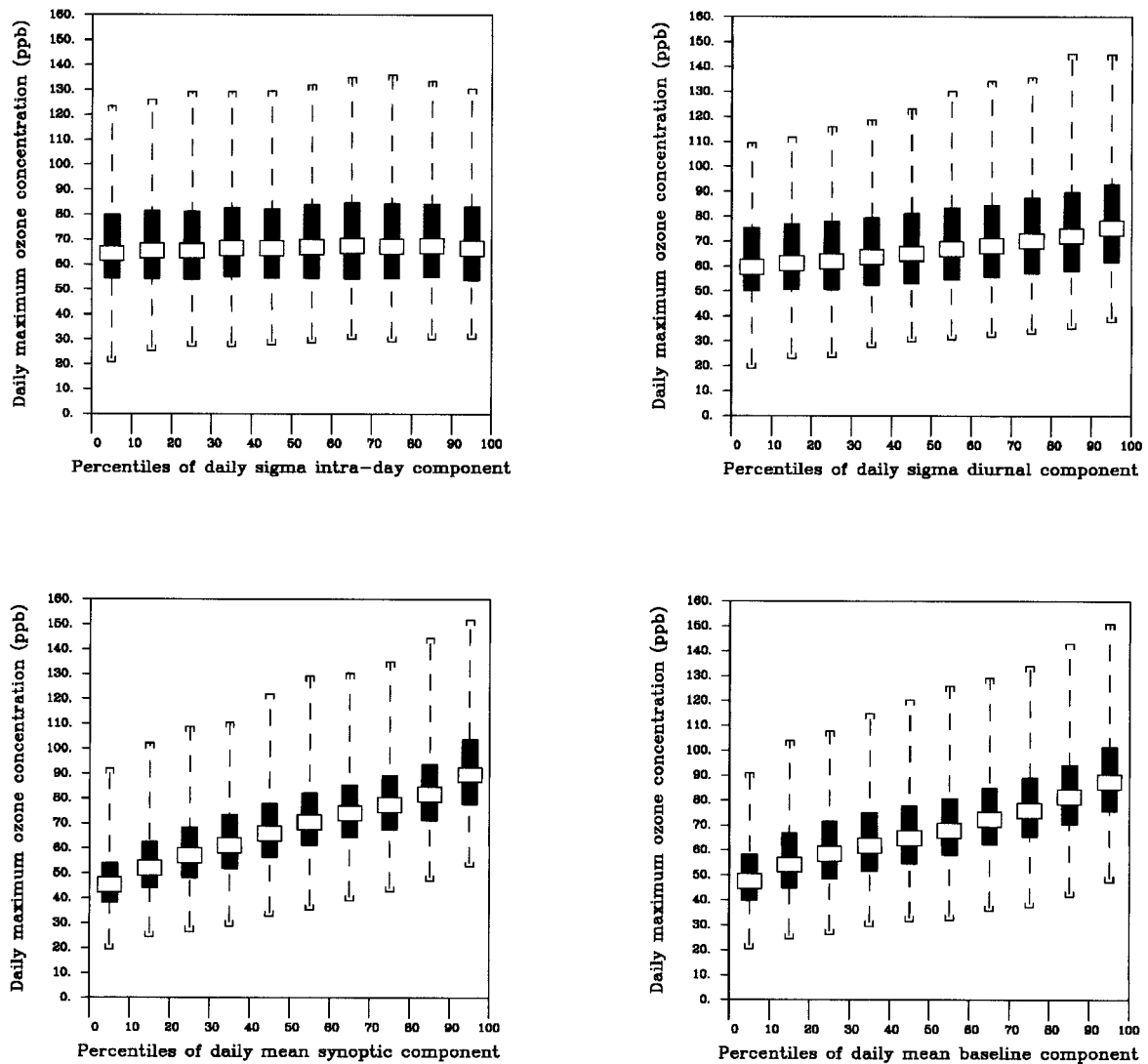


FIG. 10. As in Fig. 5, but for model predictions.

fluctuations with periods up to 21 days, and with a typical synoptic forcing on the order of 5 days, this requirement means that the modeled time period should be at least 20 days, otherwise model performance cannot be evaluated on the synoptic scale. In other words, modeling for about three weeks, while not resolving the baseline fluctuations, would at least explicitly address the fluctuations on the synoptic scale, which is one of the components that is critical to the ozone exceedances.

The simulation period needed to resolve longer-term (baseline) fluctuations with periods larger than about 20 days is on the order of 80 days. It has to be clearly understood that the modeling of periods shorter than 80 days comes at the expense of not being able to evaluate one of the key components that contributes to high ozone concentrations, and great care has

to be taken that the processes that contribute to these fluctuations and to the mean ozone concentration, such as variations of solar radiation, biogenic emissions, and variations in tropospheric background conditions, are treated adequately in the model. While baseline processes are important contributors to high ozone concentrations for the 1-h standard, an adequate treatment of baseline processes becomes even more important for the 8-h ozone standard as discussed in section 2d, since the role of longer-term forcings is more pronounced for the 8- than the 1-h standard. From a scientific point of view, a credible modeling analysis entails running the photochemical model for the entire summer season to capture the key processes that contribute to high ozone concentrations in the eastern United States. It is also clear that the previous applications of urban-scale photochemical models such as

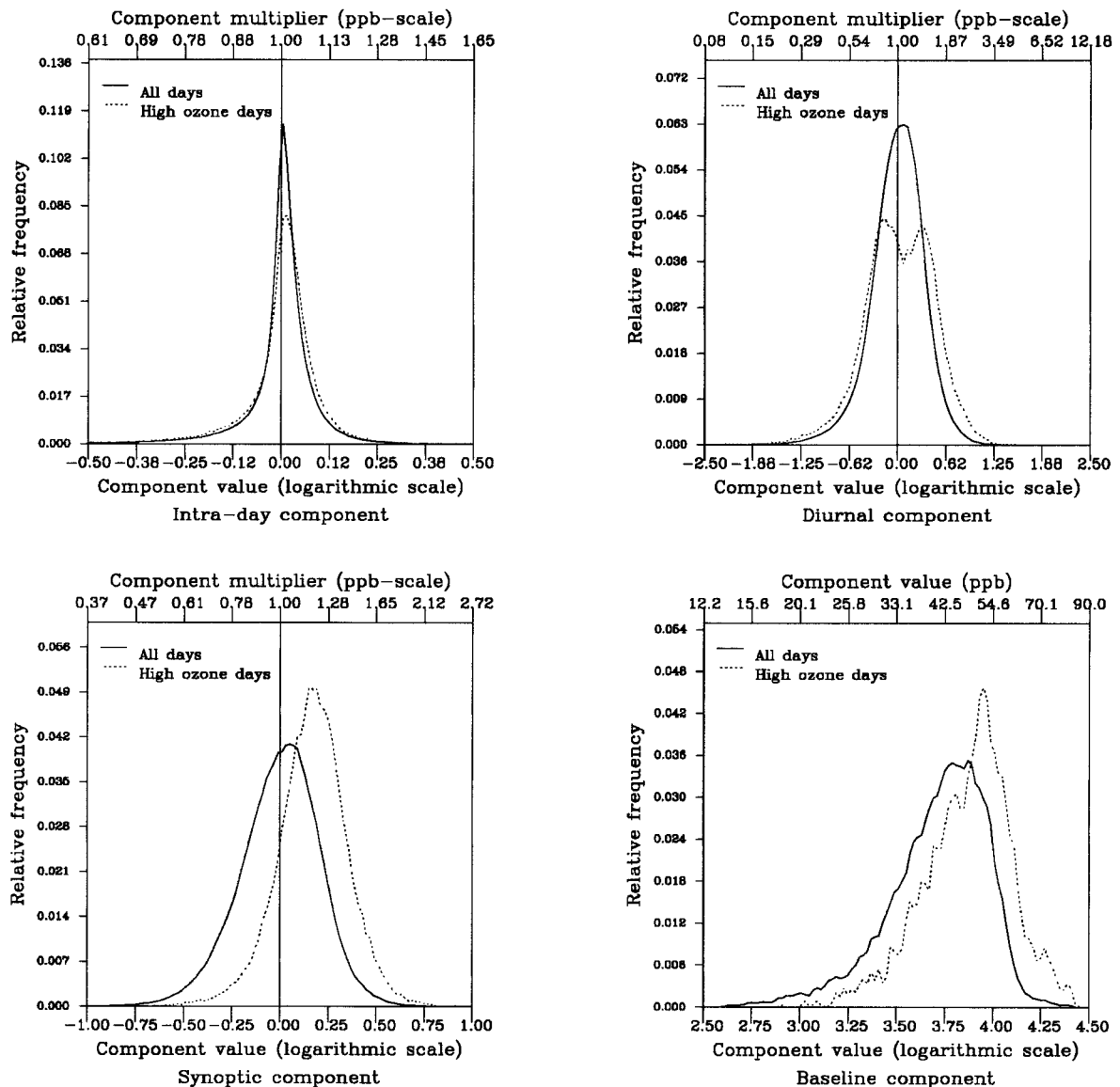


FIG. 11. As in Fig. 7, but for model predictions.

UAM-IV (U.S. Environmental Protection Agency 1990) in the past ozone attainment demonstrations did not account for the space and timescales relevant to high ozone concentrations, namely, the synoptic and baseline components and the associated spatial scales as discussed above.

f. Effects of emission reductions

The primary purpose of photochemical modeling in the regulatory framework is to assess the effects of emission reductions on simulated ozone concentrations. Using the results from a seasonal UAM-V simulation with a horizontal grid spacing of 12 km with two different emission scenarios (N. Meyer 1999, personal communication) as described in section 2a, we exam-

ine the effect of these emission reductions on the magnitude of the different temporal components. The results of this analysis are presented in Figs. 13a and 13b, which show the standard deviations and the reduction of the standard deviations (i.e., the difference between the two columns in the first diagram), respectively, for each component for the 2007 base case as well as the 2007 budget case. For the baseline, both standard deviations and the mean values are displayed. The numbers presented here are for the Greenbelt, Maryland monitor, but our conclusions are valid even if spatial average numbers are used. The differences between the 2007 base case and 2007 budget case displayed in Fig. 13b, when multiplied by 100, correspond to the percentage reduction of ozone concentrations attributable

to the reduction of the different forcings. To contrast the effects of the 2007 budget case, in which a large part of the emission reductions is due to the reduction of NO_x emissions from point sources, with a different hypothetical emission reduction scenario, Fig. 13c presents the results for a sensitivity study in which all anthropogenic NO_x emissions were uniformly reduced by 50% and all anthropogenic VOC emissions were uniformly reduced by 25%, as described in section 2a.

Two main conclusions can be drawn from this analysis. First, most of the reduction, or ozone improvement, for the 2007 budget case occurs on longer timescales, while the magnitude of the intraday component is virtually unchanged. This is an interesting finding, since this emission control strategy is aimed at reducing the regional-scale transport of ozone and its precursors as identified in the OTAG process (OTAG 1997), especially by reducing NO_x emissions from point sources. Indeed, most of the reduction occurs on the longer timescales. On the other hand, the sensitivity study in which all anthropogenic emissions were reduced by a fixed “across-the-board” or uniform percentage (Fig. 13c) shows most of the reduction on the diurnal component, pointing to a higher degree of local-scale controls in this case. Therefore, the effects of a real-world emission control strategy on the longer timescales in contrast to the effects of a hypothetical uniform emission control strategy further emphasize the importance of longer time scales to policy making. Second, and more generally, emission reduction scenarios can affect different temporal components differently. Therefore, since the results in section 3b have shown that specific situations with high ozone concentration are characterized by a specific combination of positive forcings from the diurnal, synoptic and baseline components, the amount of ozone reduction will be different from day to day or episode to episode. This is because the reduction

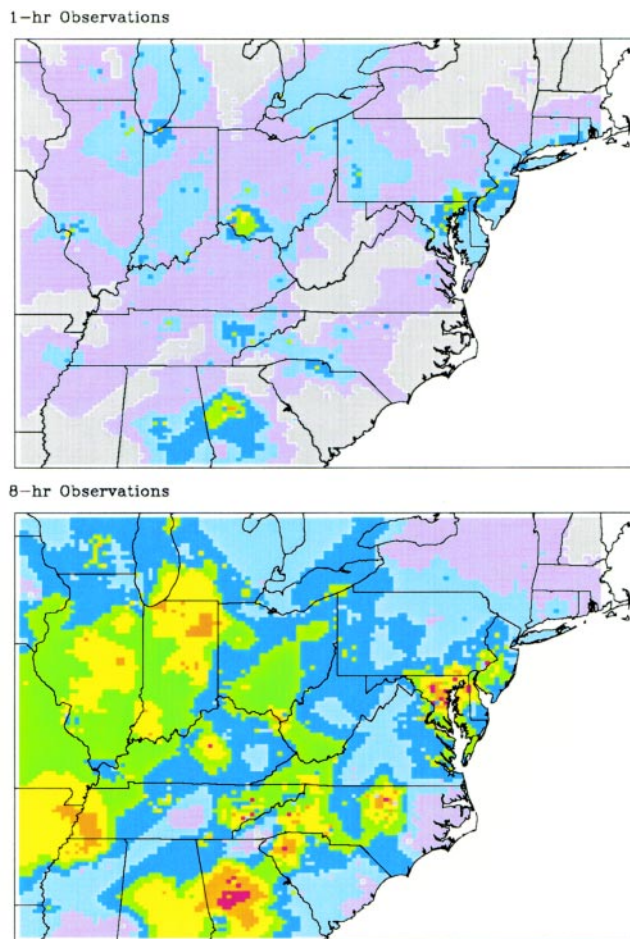


FIG. 12. Number of consecutive days for 1- and 8-h concentrations having an ozone exceedance potential as defined in the text.

on any given day will be determined by the combined effects of a reduction of the mean and a reduction of the magnitude of the different components, and by the relative importance of the different components in this specific situation.

In its recent draft modeling guidance, the U.S. EPA defined the relative reduction factor (RRF) as the ratio of the mean daily ozone maxima for the emission control and base cases (U. S. Environmental Protection Agency 1999). To determine whether the simulated emission reductions would lead to compliance with the NAAQS at a given location, observed daily maxima would be multiplied by the RRF.

Again using the results from the seasonal UAM-V simulation with the 2007 base case and 2007 budget case scenarios (N. Meyer 1999, personal communication) as described in section 2a, we can examine uncertainties associated with the RRF approach and the relationship between the RRF and the simulation time period. Typically, simulations would be carried out for

time periods having the highest observed ozone concentrations (i.e., episodic days only). Since the seasonal UAM-V simulation provides 89 days of ozone simulations, one can subset this information to mimic 89 one-day simulations, 88 two-day simulations, and so on. For a given location and simulation period, we therefore calculate a “centered” RRF. This centered RRF allows us to study the effect of simulation length on the variability of the RRF estimate and is defined as follows:

$$\text{RRF} = \frac{\bar{O}_{\text{control,max}}}{\bar{O}_{\text{base,max}}}$$

$$\bar{O}_{\text{base,max}} = \frac{\sum_{i=-n/2}^{i=n/2} o_{i,\text{max}}}{n} ; \quad \bar{O}_{\text{control,max}} = \frac{\sum_{i=-n/2}^{i=n/2} o_{i,\text{max}}}{n}$$

$$\% \text{ reduction} = 100 (1 - \text{RRF}),$$

where \bar{O}_{base} and \bar{O}_{control} are the mean of daily maximum values for base and control cases, respectively, for a given simulation length, n (say 1, 7, 13, or 21 day window etc). Obviously, for a 1-day simulation length there is no actual averaging (the RRF for any day is just the fraction of daily maximum control case to daily maximum base case for this day), and for the 7-13-, and 21-day windows, the number of averaging days is reduced near the beginning and end of the time record. For example, the 7-day percentage reduction for Greenbelt for 6 June was calculated by using daily maximum ozone concentrations from 4 June (first day of simulation) to 9 June, the 7-day percentage reduction for 7 June was calculated using daily maximum ozone values from 4 to 10 June, the 7-day percentage for 8 June was calculated using daily maximum ozone concentrations from 5 to 11 June, and so on. Note that while the RRF method was proposed for the promul-

gated 8-h standard, we applied it to both 1- and 8-h daily maximum concentrations for the following analysis and found virtually no impact on the results. The results presented are for the 1-h daily maximum concentrations.

Time series of centered percentage ozone reductions from theoretical, 1-, 7-, 13-, and 21-day simulations for the grid cell that contains the Greenbelt, Maryland station, illustrate that 1-day simulations would yield reduction factors that vary highly from day to day and, consequently, depend strongly upon the day being simulated (Fig. 16). The variability decreases as the simulation length increases. The dashed lines in Fig. 14 mark the three major ozone episodes. For these episodes, percentage reductions range between 3% and 16% for 1-day simulations, 3% and 10% for 7-day simulations, 4% and 9% for 13-day simulations, and 6% and 8% for 21-day simulations.

The dependence of the variability of the ozone reduction on the simulation length is further

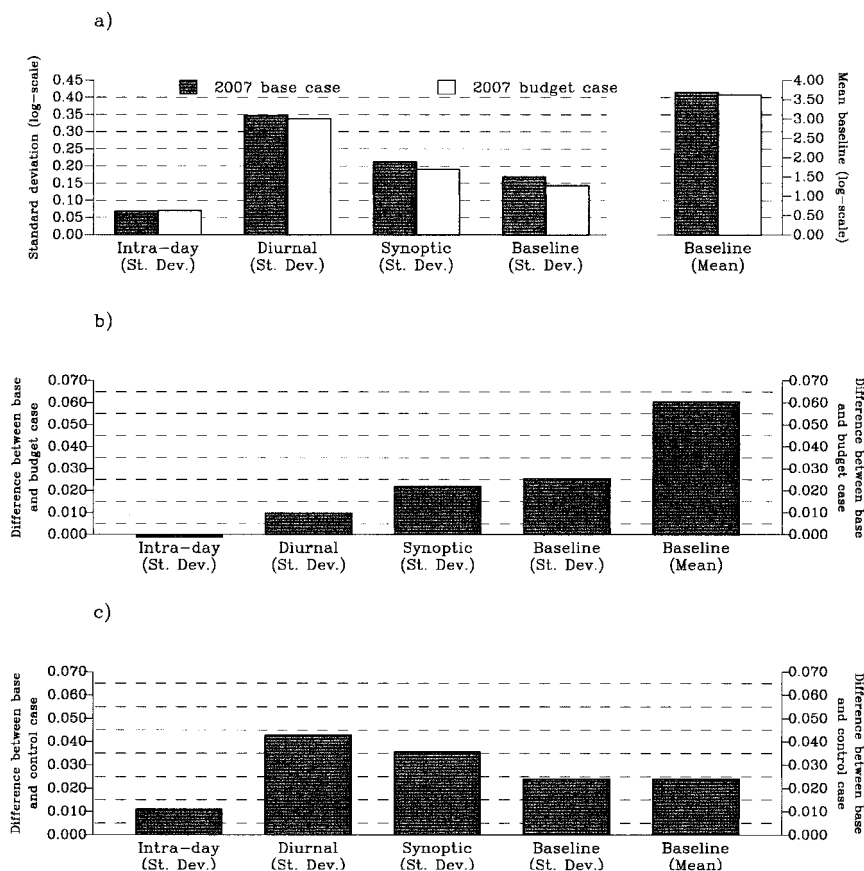


FIG. 13. (a) Standard deviation of intraday, diurnal, synoptic, and baseline components and mean for baseline component for 2007 base case and 2007 control case simulation. (b) Difference in standard deviations between the two simulations in (a) for each component and difference in means for baseline component. (c) As in (b), but for the difference between the 1995 base case and a hypothetical control case with anthropogenic NO_x emissions reduced by 50% and anthropogenic VOC emissions reduced by 25%.

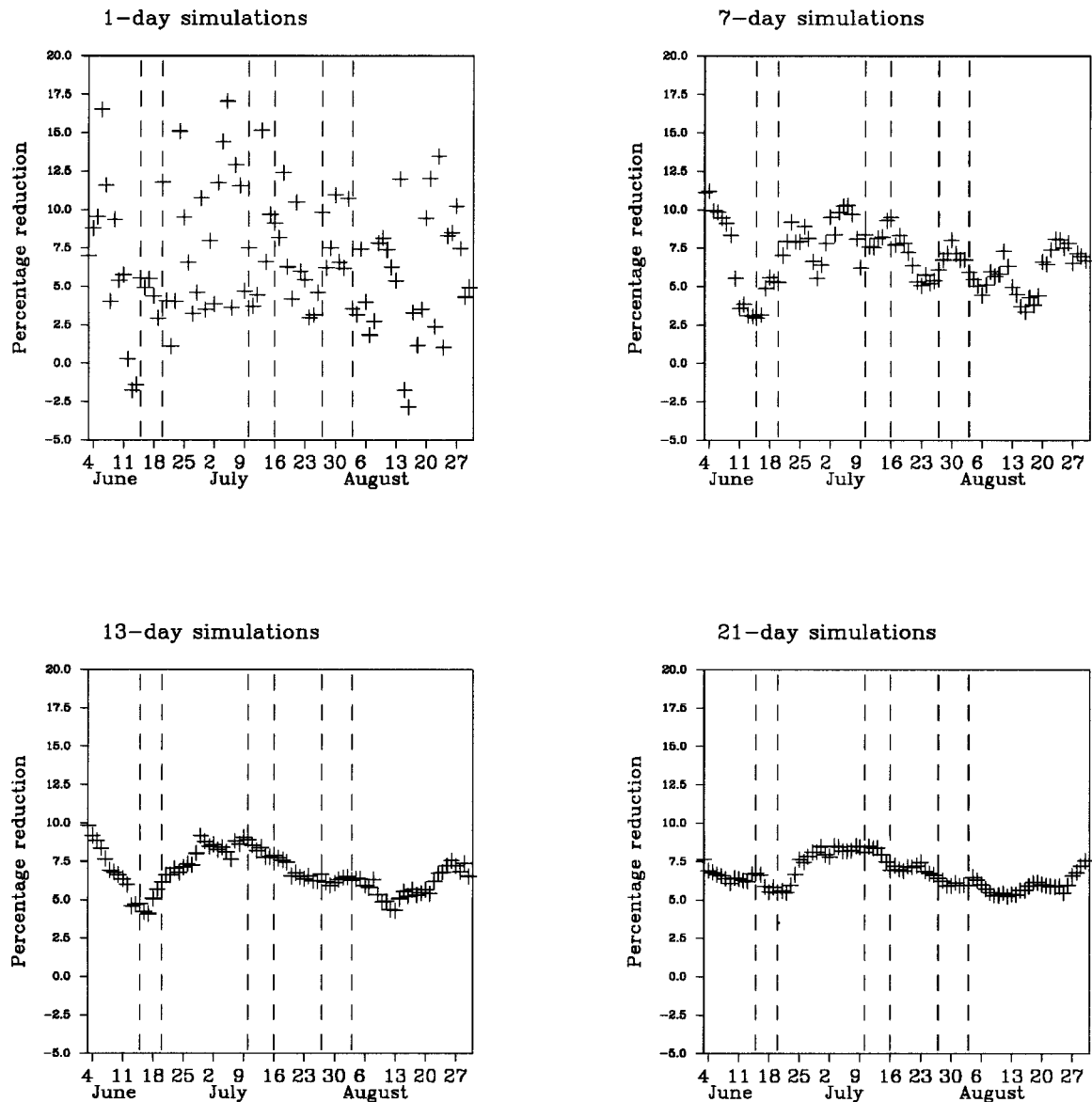


FIG. 14. Time series of relative reduction factors for Greenbelt, MD, for different simulation lengths for 4 Jun 1995–31 Aug 1995.

illustrated in Fig. 15. This figure presents a spatial image of the mean ozone reduction factor, spatial images of the associated standard deviations for 1-day, 7-day, 13-day, and 21-day simulations, and spatial images indicating whether the mean reduction is statistically significant at the $2\text{-}\sigma$ (std dev) level for a given simulation length. It is clear that reduction factors obtained from 1-day simulations hardly have any statistical significance anywhere. Although 7-day simulations lead to a large increase in the variability of the ozone reduction factors, even longer simulation periods are needed to reduce the variability of the reduction factors in the New York City and Pittsburgh areas to a

level at which the reduction factors become statistically significant.

In conclusion, it is clear that the estimates of RRF are highly variable for short simulation lengths. This variability of the RRF estimate is a function of the simulation length and decreases as the simulation length increases (which, by the definition of the RRF, also implies that the RRF estimates are the results of base and control case concentrations that are averaged over a longer time period). In other words, it is important that the concept of RRF is applied to longer modeling periods rather than episodic modeling to reduce the dependence of the RRF estimates on the selected

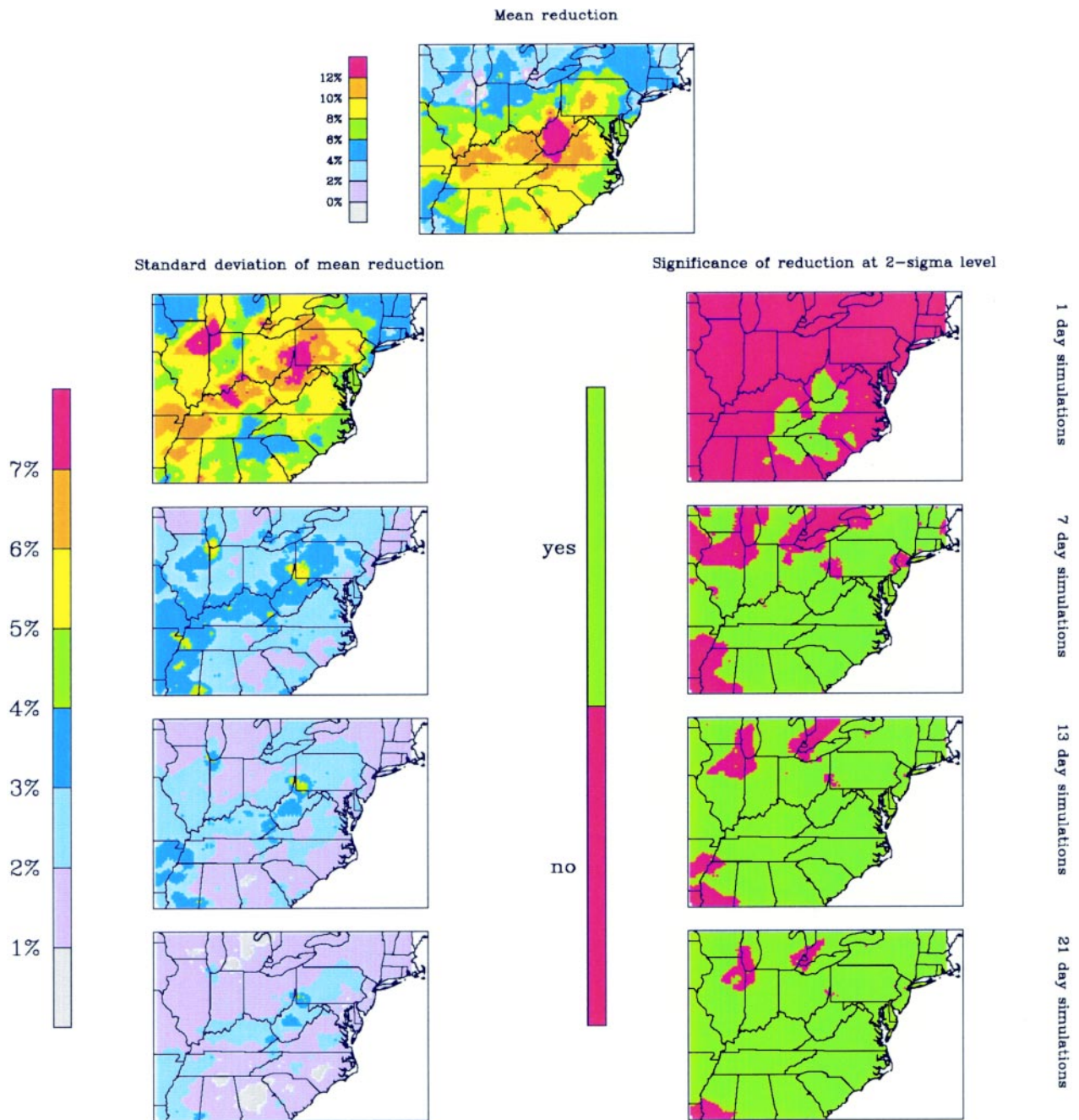


FIG. 15. Spatial images of mean relative reduction factor and standard deviation of relative reduction factor for different simulation lengths along with maps indicating whether the reduction factor is significant at the 2- σ level for a given simulation length.

modeling period. In addition, when RRFs are used in the regulatory setting, it should be clearly understood that they are subject to variability depending on the simulation period selected and ought to be accompanied by confidence limits. It is possible to estimate such confidence limits only when modeling simulations are carried out for extended time periods. If policy decisions were to be based upon one RRF for one episode only without accounting for the associ-

ated variability, there is a danger that hoped-for results can be achieved by selectively choosing the episodes or simulation lengths or “tuning” the model.

4. Summary

Days of high ozone concentrations are in general characterized by positive forcings from fluctuations

having periods equal to or greater than a day (i.e., the diurnal, synoptic, and baseline components). Fluctuations on the intraday timescale have a similar magnitude on average days and high ozone days. The particular contribution of the diurnal, synoptic, and baseline components to high ozone concentrations varies from episode to episode. The results from a seasonal simulation using the UAM-V modeling system suggest that the relative roles of longer-term forcings (diurnal amplitude, synoptic, and baseline components) are captured well by the model.

In addition, the 8-h ozone standard has greater temporal and spatial extent than the 1-h standard. Moreover, the ozone benefits predicted from regulatory modeling (for 2–3-day episodes) over smaller domains will be highly uncertain. Therefore, the modeling domain for the application of photochemical models needs to have a spatial extent of 2000–2500 km, with a simulation period covering at least four synoptic cycles. Modeling efforts directed toward finer spatial and temporal resolution at the expense of longer modeling periods and larger domains will only allow us to study the intraday component, which is not relevant to everyday decisions, in more detail. Although this focus may be of some interest for continued model development and exposure assessment, it would keep our attention away from the processes relevant to high ozone concentrations and hinder improvement in our ability to make any reliable statements from the efficacy of emission control strategies needed to meet and maintain the ozone standard and to improve long-term trends in ozone air quality.

Acknowledgments. This work is supported by the United States Environmental Protection Agency under Grant R825260-01-0 and the Electric Power Research Institute under Contract WO3189-12. The authors would like to thank E. E. Zalewsky, S. Y. Wu, W. Hao, Dr. G. Sistla, Dr. G. Kallos, Dr. V. Kotroni, and Dr. K. Lagouvardos for performing the model simulations and Dr. R. Henry for his help with the AIRS dataset. Thanks are extended to K. Schere of U.S. EPA and Dr. D. A. Hansen of EPRI for their critical review of the manuscript and their helpful and constructive comments. The authors would also like to thank the anonymous reviewers for helping us in improving the clarity of the paper.

References

- Bankov, E., S. T. Rao, and P. S. Porter, 1998: A trajectory-clustering correlation methodology for examining the long-range transport of air pollutants. *Atmos. Environ.*, **32**, 1525–1534.
- Chan, D., S. T. Rao, I. G. Zurbenko, and P. S. Porter, 1999: Linking changes in ozone to changes in emissions and meteorology. *Proc. Air Pollution 99 Conf.*, Palo Alto, CA, Wessex Institute of Technology, 663–675.
- Eskridge, R. E., J.-Y. Ku, S. T. Rao, P. S. Porter, and I. G. Zurbenko, 1997: Separating different scales of motion in time series of meteorological variables. *Bull. Amer. Meteor. Soc.*, **78**, 1473–1483.
- Goody, R., J. Anderson, and G. North, 1998: Testing climate models: An approach. *Bull. Amer. Meteor. Soc.*, **79**, 2541–2549.
- Hanna, S. R., G. E. Moore, and M. E. Fernau, 1996: Evaluation of photochemical grid models (UAM-IV, UAM-V, and the ROM-UAM-IV couple) using data from the Lake Michigan Ozone Study (LMOS). *Atmos. Environ.*, **30**, 3265–3279.
- Hogrefe, C., S. T. Rao, I. G. Zurbenko, and P. S. Porter, 1999a: Information in ozone observations and model predictions on different time scales. *92nd Annual Meeting of the Air and Waste Management Association*, St. Louis, MO, Air Waste Manage. Assoc., CD-ROM. [Available from A&WMA Publications Order Department, P. O. Box 1020, Sewickley, PA 15143.]
- , ——, and ——, 1999b: Seasonal photochemical modeling over the eastern United States: Model performance on different space and time scales and implications to the use of models in a regulatory setting. Preprints, *Symp. on Interdisciplinary Issues in Atmospheric Chemistry*, Dallas, TX, Amer. Meteor. Soc., 42–49.
- Lagouvardos, K., G. Kallos, and V. Kotroni, 1997: Modeling and analysis of ozone and its precursors in the northeast U.S.A. (Atmospheric modeling simulations). Final report to Electric Power Research Institute, Palo Alto, CA, 46 pp. [Available from Office of Science and Technology, NYSDEC, Room 198, 50 Wolf Rd., Albany, NY 12233-3259.]
- Lamb, R. G., 1983: A regional scale (1000 km) model of photochemical air pollution, Part 1: theoretical formulation. EPA-600/3-83-035, 239 pp. [Available from United States Environmental Protection Agency, Research Triangle Park, NC 27711.]
- McRae, G. J., and J. H. Seinfeld, 1983: Development of a second-generation mathematical model for urban air pollution. 2: Evaluation of model performance. *Atmos. Environ.*, **17**, 501–522.
- Milanchus, M. L., S. T. Rao, and I. G. Zurbenko, 1998: Evaluating the effectiveness of ozone management efforts in the presence of meteorological variability. *J. Air Waste Manage. Assoc.*, **48**, 201–215.
- OTAG, 1997: OTAG final report. [Available online at <http://www.epa.gov/ttn/rto/otag/finalrpt>.]
- Pielke, R. A., and M. Uliasz, 1998: Use of meteorological models as input to regional and mesoscale air quality models—Limitations and strengths. *Atmos. Environ.*, **32**, 1455–1466.
- Porter, P. S., S. T. Rao, I. G. Zurbenko, E. E. Zalewsky, R. F. Henry, and J.-Y. Ku, 1996: Statistical characteristics of spectrally-decomposed ambient ozone time series data. Report prepared for the Ozone Transport Assessment Group (OTAG). [Available online at <http://capita.wustl.edu/otag/reports/StatChar/otagrep.htm>.]
- , ——, ——, A. M. Dunker, and G. T. Wolff, 2000: Ozone air quality over North America: Part 2, A review of trend detection and attribution techniques. *J. Air Waste Manage. Assoc.*, submitted.

- Rao, S. T., I. G. Zurbenko, R. Neagu, P. S. Porter, J. Y. Ku, and R. F. Henry, 1997: Space and time scales in ambient ozone data. *Bull. Amer. Meteor. Soc.*, **78**, 2153–2166.
- , and Coauthors, 1998: Integrating observations and modeling in ozone management efforts. *Air Pollution Modeling and its Applications*, Vol. XII, Plenum Press, 115–122.
- , and Coauthors, 2000: An integrated modeling and observational approach for designing ozone control strategies for the eastern United States. *Air Pollution Modeling and its Applications*, Vol. XIII, S. E. Gryning and E. Batchvarova, Eds., Kluwer Academic Plenum Publishers, 3–16.
- Russell, A., and R. Dennis, 2000: NARSTO critical review of photochemical models and modeling. *Atmos. Environ.*, **34**, 2283–2324.
- Salcedo, R. L. R., M. C. M. Alvim Ferraz, C. A. Alves, and F. G. Martins, 1999: Time series analysis of air pollution data. *Atmos. Environ.*, **33**, 2361–2372.
- Systems Applications International, 1995: Users guide to the Variable Grid Urban Airshed Model (UAM-V). Systems Applications International, San Rafael, CA, 131 pp. [Available from Systems Applications International, 101 Lucas Valley Rd., San Rafael, CA 94903.]
- Tesche, T. W., D. E. McNally, J. G. Wilkinson, C. F. Loomis, and R. A. Emigh, 1996: Initial estimates of emissions reductions needed for ozone attainment in the Pittsburgh-Beaver Valley ozone nonattainment area. Report prepared for Southwestern Pennsylvania Clean Air Stakeholder Group, 113 pp. [Available from Alpine Geophysics, LLC, P. O. Box 17344, Covington, KY 41017.]
- U.S. Environmental Protection Agency, 1990: User's guide for the Urban Airshed Model (seven volumes). EPA-450/4-90-007. [Available from United States Environmental Protection Agency, Research Triangle Park, NC 27711.]
- , 1999: Draft report on the use of models and other analyses in attainment demonstrations for the 8-hour ozone NAAQS. EPA-44/R-99-0004. [Available from United States Environmental Protection Agency, Research Triangle Park, NC 27711.]
- Vukovich, F. M., 1997: Time scales of surface ozone variations in the regional, non-urban environment. *Atmos. Environ.*, **31**, 1513–1530.
- Zhang, J., and S. T. Rao, 1999: The role of vertical mixing in the temporal evolution of the ground-level ozone concentrations. *J. Appl. Meteor.*, **38**, 1674–1691.
- Zurbenko, I. G., 1986: *The Spectral Analysis of Time Series*, North-Holland, 236 pp.